

## CHAPTER I

### INTRODUCTION

Ruminants, like all mammals, have a requirement for glucose. However, glucose is not absorbed from the digestive tract of ruminants in significant quantities except under particular grain feeding situations. Therefore, on the majority of diets, ruminants depend on gluconeogenesis to supply their glucose requirements. The possibility that the supply of gluconeogenic precursors may limit production under some situations, has led to extensive investigation of the rates of conversion of potential precursors to glucose.

Isotope dilution techniques have been used in these investigations to determine precursor/glucose relationships. When using these techniques it is assumed that the metabolism of the material being traced (the tracee) can be quantified by observing the dilution of the labelled material (the tracer) in the pool into which the tracer is infused (primary pool), and its appearance in product pools (secondary pools). These techniques allow the movement of specific atoms or groups of atoms to be followed through various secondary pools. However, a flow of tracer need not always be associated with a net flow of tracee because of the effects of influences such as

1. equilibration of isotope in symmetrical compounds (section 2.2.2.1)
2. metabolic crossover (section 2.2.2.2)
3. incorporation of tracer via indirect routes (section 2.2.2.3)
4. recycling of tracer (section 2.2.2.4).

Incomplete understanding of the metabolism of the tracer has led, at times, to estimates of tracer flows being interpreted mistakenly as indicating net tracee flows.

In this thesis, the interpretation of data from isotope dilution experiments designed to investigate the contribution of propionate to glucose is evaluated. This evaluation allows the effects of 1 to 4 above to be illustrated. It is shown that failure to account for these effects will lead to serious errors in the estimate of the true contribution of propionate to glucose. In particular, the effects of metabolic crossover have not always been fully appreciated and accounted for in the interpretation of such data.

It has long been known that acetate carbon can be incorporated into glucose even though there is no net flow of acetate carbon to glucose (Weinman, Strisower and Chaikoff 1957). Acetate carbon is incorporated into glucose through exchange of molecules between gluconeogenic pathways and intermediates of the tricarboxylic acid cycle (i.e. metabolic crossover). This exchange of molecules will not affect the net flows, but will decrease the amount of tracer in the glucose pathway. If X% of glucose molecules are provided by acetate derived oxaloacetate molecules then the incorporation of oxaloacetate molecules derived from net precursors of glucose will be

decreased by X%. As will be discussed in section 7.3.3, 9.3% and 12.6% of glucose carbons 3 and 4 were provided by the carboxyl carbon of rumen acetate in sheep fed 800g/d oaten straw. Pethick, Lindsay, Barker and Northrop (1981), (using a different diet) found that even if all the acetate taken up by the liver was oxidized, acetate could only account for 30% of the oxygen uptake. Thus, other substrates also are important suppliers of acetyl-CoA for oxidation in the tricarboxylic acid cycle in the liver. Therefore, these other substrates are also suppliers of acetyl-CoA that enters the tricarboxylic acid cycle and thus provide carbon for oxaloacetate molecules that can exchange with those in the gluconeogenic pathways.

Bergman (1973) presented data that suggested that the percentage of glucose being provided by propionate estimated by the conversion of  $^{14}\text{C}$ -propionate to glucose was only 67% the estimate from net hepatic uptake of propionate. However, Lindsay (1978) presented data that suggested that the two methods of estimation gave similar results. Unfortunately, the two methods of estimation have not been used in the same animals and therefore, because of the apparent variability of propionate production, the comparisons could be misleading. The incorporation of tracer from acetate can not be explained without postulating the occurrence of metabolic crossover.

It is hypothesised that failure to account for the effects of metabolic crossover would cause estimates of the percentage of glucose carbon provided by propionate, based on the incorporation of propionate tracer, to lead to a serious underestimation of the net contribution of propionate to glucose carbon. This error in interpretation would have important consequences in glucose balance studies, for if a reinterpretation of the data indicated that a

greater proportion of the glucose irreversible loss was coming from propionate, then this would reduce the amount assigned by difference as coming from amino acids. It has been suggested that amino acids are major precursors of glucose but it has been difficult to understand why the ruminant would use protein for gluconeogenesis if excess propionate were available. Reinterpretation of existing data with a correction for the effects of metabolic crossover may help resolve this important question.

CHAPTER 2  
ISOTOPE KINETICS

2.1 ISOTOPE DILUTION

The availability of instruments capable of measuring minute concentrations of isotope tracers has led to isotopes being used extensively in studying biological systems. The quantity of tracer that has to be introduced into the system under investigation to give statistically acceptable counting rates is negligible compared to the mass of tracee in that system and thus should not perturb the characteristics of the system.

Various techniques have evolved for the administration of radioisotopes and for the mathematical treatment of the data subsequently obtained. A number of terms are used to describe the distribution, rate of movement and dilution of tracer in the system under investigation. The following terms are used in this thesis.

A POOL or COMPARTMENT of tracee is a mass of material of isokinetic behaviour, in which tracer, if present, is homogeneously mixed. (The mathematical analysis of isotope dilution data is based on the assumption that tracer introduced into a given compartment mixes instantaneously).

A SYSTEM of tracee is composed of several pools among which interconversions of molecules occur.

CONTINUOUS INFUSION refers to the infusion of a small quantity of tracer at a precisely controlled rate.

STEADY STATE is when the rates of removal and replacement of tracee are equal, i.e. the total amount of tracee in the compartment is constant during the period of observation. The assumption of steady state in the system is implicit in the following definitions and for the mathematical analysis of the isotope dilution data.

The SPECIFIC RADIOACTIVITY of the material in a pool is the radioactivity per unit of mass of tracee.

PLATEAU specific radioactivity refers to the estimated value of the asymptote which is approached by the ratio of tracer to tracee during a continuous infusion of the tracer into a pool.

The TRANSFER QUOTIENT is the plateau specific radioactivity in the product pool divided by the plateau specific radioactivity in the tracee pool during a continuous infusion of tracer.

TOTAL ENTRY RATE is the rate (mass/unit time) at which tracee enters or leaves a compartment under steady state conditions. The rate of IRREVERSIBLE LOSS is the rate (mass/unit time) at which tracee leaves a pool and does not return during the period of observation (calculated by dividing the infusion rate of tracer by the plateau specific radioactivity of the pool into which the tracer is infused). These definitions embody the concept of RECYCLING, a process whereby a proportion of the tracee which has left a pool returns to that pool during the period of observation.

GENERAL MODEL refers to an open system of pools in steady state. Each general model completely represents total inflows and outflows and all possible interactions between the pools identified, and the whole animal system of which these compartments are a part (Nolan, Norton and Leng, 1976). MODEL refers to the system of pools where one or more of the flows have been deleted for theoretical biological reasons. All of the flows in the models represent the overall effect of possibly numerous individual routes of transfer.

ENTRY RATE refers to the rate of entry of material into a pool in the model calculated by addition of all the inflows to that pool. Some, but not necessarily all of, the recycling of tracer may be accounted for. Thus, this value may be intermediate between the total entry and the irreversible loss rate estimates.

## 2.2 INTERPRETATION OF TRANSFER QUOTIENTS

### 2.2.1 Introduction

In experiments utilizing isotope dilution techniques, the conversion of one metabolite to another is usually estimated as the transfer quotient. The transfer quotient is the proportion of the traced atoms in the product pool that originated in the tracee pool. In many instances this proportion is the net proportion of the product pool provided by the tracee pool. However, depending on the metabolite, there may be tracer flows that are not associated with net tracee flows. In these circumstances, the transfer quotient is not the proportion of the product pool provided by the tracee pool. Some of these circumstances are discussed below.

## 2.2.2 Situations Where Tracer Flows Are Not Associated With Net Tracee Transfer

### 2.2.2.1 Symmetrical Compounds -

Some symmetrical compounds have more than one orientation by which they can combine with their enzymes. This can cause a change in the intramolecular distribution of tracer in all compounds in the pathway forward of this point, thus causing the labelling pattern of a product to change without changing the net flows.

An example of the effects of a symmetrical compound in a pathway bringing about tracer flows not associated with net flows is the incorporation of  $^{14}\text{CO}_2$  into glucose (explained in detail in Section 4.5).

### 2.2.2.2 Dilution Caused By Metabolic Crossover -

Oxidation of acetate via the tricarboxylic acid cycle involves condensation of acetyl-CoA with oxaloacetate to form citrate. Two molecules of  $\text{CO}_2$  are lost as this citrate is reconverted to oxaloacetate by the tricarboxylic acid cycle pathway. No net increase in pool size of any of the intermediates results from complete turns of the tricarboxylic acid cycle. Therefore, at steady state, for every molecule that enters the oxaloacetate pool from the tricarboxylic acid cycle, a molecule must leave via condensation with acetyl-CoA to continue cycling.

There are metabolic pathways that form intermediate pools in common with the tricarboxylic acid cycle. As molecules within a pool are indistinguishable (with respect to the origin of the molecules in the pool), all flows from that pool must have the same composition



(i.e. the same specific radioactivity). Thus, the proportion of the oxaloacetate pool provided by any inflow is the proportion which that inflow contributes to any outflow. For example, if an inflow provides 10% of the oxaloacetate pool, it must provide 10% of the material in every flow out of the oxaloacetate pool. Thus, molecules from pathways that are net inputs to intermediate pools of the tricarboxylic acid cycle crossover or exchange with molecules that were formed by the reactions of the cycle. This exchange decreases the amount of radioactivity in the material (i.e. decreases the specific radioactivity) in the net input pathway forward of the pool that is in common with the tricarboxylic acid cycle.

The crossing over or exchange of molecules between the tricarboxylic acid cycle and other pathways is referred to as "metabolic crossover". It causes the pattern of actual molecule flow (tracer flow) to differ from the pattern of net molecule flow (Krebs, Hems, Weidemann and Speake, 1966; Vinay, Mapes and Krebs, 1978). Therefore, when using isotope dilution techniques to quantify the contribution of a precursor to product, the dilutions brought about by metabolic crossover must be accounted for, otherwise the transfer quotient will underestimate the net flow from precursor to product.

#### 2.2.2.3 Tracer Incorporation Via Indirect Routes -

The transfer quotient does not take into account the pathway of tracer incorporation. Unless more than one pathway is known to be operative, it is normally assumed that most, or all of the tracer is incorporated into the product via the main route. However, if other secondary pools become labelled, the tracer flow via indirect routes through these other secondary pools may be significant. This would

lead to an overestimation of the flow along the assumed route. As discussed in Section 7.3.3 some 50% of the tracer in glucose when [1-<sup>14</sup>C]acetate was infused intraruminally was in glucose due to interaction with the bicarbonate pools.

#### 2.2.2.4 Recycling Of Tracer -

Cycling of tracer back to an intermediate pool in a pathway will increase the specific radioactivity of that pool above that resulting from tracer inflow direct from the pool into which the tracer was infused. Compounds forward of this pool will have this increased specific radioactivity. For example, if the oxaloacetate pool was being labelled by [2-<sup>14</sup>C]propionate, some labelled molecules would be entering the tricarboxylic acid cycle. As no tracer in oxaloacetate from [2-<sup>14</sup>C]propionate is lost on the first turn of the cycle, tracer is returned to the oxaloacetate pool and thus, raises its specific radioactivity. Any product synthesized from oxaloacetate will have this raised specific radioactivity. Thus, recycling of tracer can cause the transfer quotient to overestimate the flow along the direct route.

## CHAPTER 3

### PROPIONATE METABOLISM

#### 3.1 INTRODUCTION

Propionate is one of the major volatile fatty acids produced by fermentation in the rumen. It is the only one of the major volatile fatty acids that can give rise to net amounts of glucose, and is used extensively for this purpose by ruminant animals. The pathway from propionate to glucose has intermediate pools in common with the tricarboxylic acid cycle and thus, metabolic crossover will affect the incorporation of tracer from propionate into glucose.

In this chapter the metabolism of propionate is discussed. Firstly, the biochemistry of the propionate molecule is given. This is followed by a discussion of the metabolism of the carboxyl and middle carbons of propionate with emphasis on the differences between tracer and net carbon flows.

## 3.2 PROPIONATE METABOLISM (WHOLE MOLECULE)

### 3.2.1 Formation Of Propionate In The Rumen

Two routes of propionate formation have been found in pure cultures of anaerobic bacteria: the dicarboxylic acid pathway and the direct reductive pathway (Baldwin, 1965).

In the dicarboxylic acid pathway, the 3 carbon units, pyruvate or phosphoenolpyruvate are carboxylated to form oxaloacetate or malate respectively. Malate is dehydrated to form fumarate. Fumarate is reduced to form succinate, activated to succinyl-CoA, isomerised to methylmalonyl-CoA, then decarboxylated to form propionyl-CoA.

In propionibacteria the latter reaction is catalysed by a biotin containing transcarboxylase which transfers the "activated" CO<sub>2</sub> derived from methylmalonyl-CoA to pyruvate, forming propionyl-CoA and oxaloacetate. The advantage of this is that there is no requirement for energy (ATP) to drive the pathway. The succinate decarboxylation system of Vibrio alcalescens appears to differ from that of the propionibacteria in that the "activated" CO<sub>2</sub> derived in the decarboxylation step is not bound as tightly and is readily released as CO<sub>2</sub>. If this occurs, energy is needed to carboxylate pyruvate, the initial reaction of the pathway (Baldwin, 1965).

The conversion of lactate to propionate via the direct reductive pathway involves activation of lactate to form lactyl-CoA, dehydration of the lactyl-CoA to acrylyl-CoA and reduction to form propionyl-CoA (Baldwin, 1965). The relative contribution of each pathway is diet dependent, with the reduction pathway becoming more prominent as the carbohydrate availability of the diet increases (Baldwin, 1965).

### 3.2.2 Absorption Of Propionate From The Rumen

There has been some controversy about the fate of propionate during absorption from the rumen. In vitro systems have shown that rumen mucosa can extensively convert propionate to lactate (Pennington and Sutherland, 1956). However, Weekes and Webster (1974) found that the rate of lactate formation by the portal drained viscera was not affected by infusions of high or low propionate mixtures into the rumen. Weigand, Young and McGilliard (1972) found that less than 5% of the propionate (after correction for the flow of tracer from propionate via glucose to lactate) was converted to lactate in the ruminoreticulum epithelium in vivo. They found that propionate plus the small amounts of lactate were sufficient to account for all the portal-arterial difference in total radioactivity and suggested that most, if not all, of the propionate absorbed from the ruminoreticulum was transported into the portal system as propionate or lactate. Weekes (1972) calculated, using measurements from in vitro incubations of rumen papillae, that the extent of conversion of propionate absorbed from the rumen into pyruvate and lactate was small (averaging 3%) and thus supported the work of Weigand et al. (1972). Weekes and Webster (1974) reported that if glucose taken up by the portal drained viscera was metabolized through the glycolytic pathway, the production of lactate could be accounted for.

### 3.2.3 Metabolism Of Propionate In The Liver

Cellular membranes are freely permeable to volatile fatty acids; therefore, the volatile fatty acids must be trapped within the cell for subsequent metabolism to occur. This is achieved by conversion to an impermeable CoA derivative by an 'activation reaction' catalysed by

acyl-CoA synthetases (Ricks and Cook, 1981).

Ricks and Cook (1981) found that mitochondria of bovine liver contain a propionyl-CoA synthetase of high specificity for propionate and a butyrate activating fraction with broad substrate specificity. They suggested that at normal or lower propionate concentrations propionyl-CoA synthetase could activate all propionate presented to the liver. When larger amounts of propionate are presented to the liver the butyrate activating enzyme would also become important in activating propionate. It has been found that almost all propionate is removed from portal blood in its first pass through the liver (Annison, Hill and Lewis, 1957; Bergman, Roe and Kon, 1966).

Following activation, propionyl-CoA undergoes enzymic carboxylation to form the D-isomer of methylmalonyl-CoA. The reaction is catalysed by propionyl-CoA carboxylase. This enzyme contains a covalently attached prosthetic group, biotin, which serves as a carrier of 'activated' CO<sub>2</sub>. A bicarbonate molecule becomes attached to the biotin-enzyme at the expense of ATP. In a subsequent reaction the 'activated' carboxyl group is transferred to propionyl-CoA to form D-methylmalonyl-CoA (Stryer, 1981). The D-isomer of methylmalonyl-CoA is then 'racemized' to the L-isomer.

Succinyl-CoA is formed from L-methylmalonyl-CoA by intramolecular rearrangement. The CO-S-CoA group migrates from carbon 2 to carbon 3 in exchange for a hydrogen atom. This reaction is catalysed by methylmalonyl-CoA mutase which contains a derivative of cobalamin (vitamin B<sub>12</sub>) as its co-enzyme (Stryer, 1981).

Succinyl-CoA is converted to succinate by cleavage of the thioester bond by succinyl-CoA synthetase. Succinate is oxidized to fumarate by succinate dehydrogenase. Malate is then formed by fumarase catalysing a stereospecific transhydration of fumarate. Malate is oxidized to oxaloacetate by malate dehydrogenase. The four dicarboxylic acids (succinate to oxaloacetate) appear to be in reversible equilibrium (Hoberman and D'Adamo, 1960).

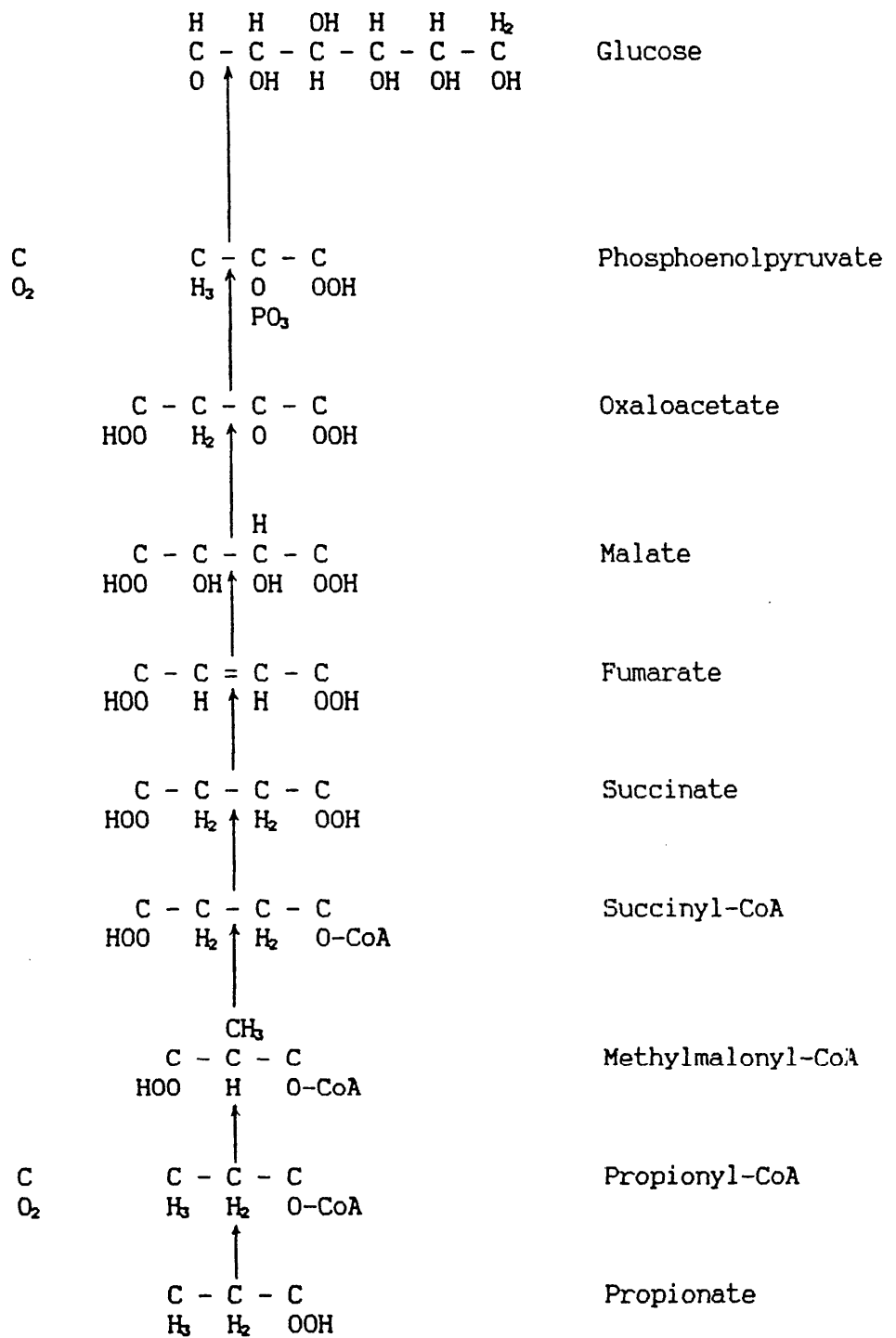
Glucose is formed from oxaloacetate via the following pathway. Oxaloacetate is converted to phosphoenolpyruvate by phosphoenolpyruvate carboxykinase. Two phosphoenolpyruvate molecules are joined and converted to fructose 1,6-diphosphate by reversal of the glycolytic pathway. Fructose 1,6-diphosphate is converted to fructose 6-phosphate by the action of fructose 1,6-diphosphatase. The fructose 6-phosphate is reversibly converted to glucose 6-phosphate by phosphohexoisomerase. This can then be converted to free glucose via the action of glucose 6-phosphatase. A schematic diagram of the pathway by which propionate is converted to glucose is shown in Figure 3-1.

#### 3.2.4 Intracellular Location Of The Enzymes Which Convert Propionate To Glucose

The initial enzymes of the pathway between propionate and glucose are intramitochondrial while those involving reversal of glycolysis are cytosolic. Therefore, intermediates must pass through the mitochondrial membrane. At exactly what stage this occurs has been the subject of some controversy, but it appears to occur between malate and phosphoenolpyruvate.

Figure 3-1

A schematic diagram of the pathway by which propionate is converted directly to glucose





There is considerable species variation in the intracellular distribution of phosphoenolpyruvate carboxykinase (Soling and Kleineke, 1976). Taylor, Wallace and Keech (1971) found that there were considerable amounts of phosphoenolpyruvate carboxykinase activity in both the mitochondria (30%) and cytosol (70%) of sheep. Both cytosolic and mitochondrial phosphoenolpyruvate carboxykinase appear to be involved in gluconeogenesis because they respond similarly to factors (diabetes and starvation) that affect glucose formation (Taylor et al., 1971).

The mitochondrial membrane appears to be freely permeable to phosphoenolpyruvate formed in the mitochondria. However, the rates of oxaloacetate movement from the mitochondria are not sufficient to account for the reaction rates of cytosolic phosphoenolpyruvate carboxykinase (Ballard, Hanson and Kronfeld, 1969). Therefore, other ways of supplying oxaloacetate for cytosolic phosphoenolpyruvate carboxykinase must exist. One way by which this is achieved is for molecules to leave the mitochondria as malate. These molecules are subsequently oxidized to oxaloacetate in the cytosol by malate dehydrogenase. The advantage of this is that reducing equivalents (NADH) are generated in the cytosol where they are needed for a later step in the glucose pathway. Another possible method is for oxaloacetate to leave the mitochondria as aspartate (Walter, Paetkau and Lardy, 1966). This method does not involve the transfer of reducing equivalents (Hanson, 1974). The flux through each of the above pathways depends on the redox state of the compartments within the cells (Brosnan, 1982).

### 3.3 PROPIONATE TRACER METABOLISM - [2-<sup>14</sup>C]PROPIONATE

#### 3.3.1 The Positions Of The Carbon Atoms In The Intermediates Which Become Labelled When [2-<sup>14</sup>C]propionate Is Converted Directly To Glucose

The positions of the carbon atoms in the intermediates which become labelled when [2-<sup>14</sup>C]propionate is metabolised directly to glucose are shown in Figure 3-2. Succinate and fumarate are symmetrical compounds and, therefore, can be accepted by their respective enzymes in either of two orientations. This results in tracer being distributed equally about both middle carbons of the dicarboxylic acids and carbons 2 and 3 of phosphoenolpyruvate. As a glucose molecule is formed via the joining of 2 molecules derived from phosphoenolpyruvate, carbon in positions 1, 2, 5 and 6 of glucose become labelled. No tracer is incorporated into carbons 3 or 4 of glucose by the direct pathway shown in Figure 3-2. In the following discussion oxaloacetate will be used as an example of the dicarboxylic acids.

#### 3.3.2 Effect Of Metabolic Crossover On Interpretation Of The Transfer Quotient When [2-<sup>14</sup>C]propionate Is Converted To Glucose

##### 3.3.2.1 Dilution Of Tracer -

The enzymes that catalyse the reactions involved in the conversion of succinate to oxaloacetate are enzymes of the tricarboxylic acid cycle. Therefore, oxaloacetate derived from cycling of the tricarboxylic acid cycle mixes with oxaloacetate derived from propionate, as evidenced by acetate carbon being incorporated into glucose (Weinman et al., 1957). Thus, the specific



radioactivity of the oxaloacetate pool is lower than it would be if the mixing did not occur. As this metabolic crossover dilution occurs without changing the net flow of molecules to glucose, it causes the transfer quotient to underestimate the percentage of glucose being provided by propionate.

### 3.3.2.2 Recycling Of Tracer In The Tricarboxylic Acid Cycle -

When an oxaloacetate molecule labelled by [2-<sup>14</sup>C]propionate enters and completes a single turn of the tricarboxylic acid cycle both methyl carbons (and therefore all the tracer) return to the oxaloacetate pool. However, because succinate is symmetrical the tracer is effectively distributed equally about all 4 carbon positions (Fig 3-4). Figure 3-3 shows the molecules whose carbon skeletons only are presented in Figures 3-4, 5, 7 and 4-1 and 4-2. If this molecule goes round the cycle again, the tracer on the carboxyl carbons (half the tracer) is removed. The tracer on the methyl carbons equilibrates about the carbons of succinate and returns to the oxaloacetate pool again (Figure 3-5). On all subsequent turns of the tricarboxylic acid cycle, half the remaining label is lost and the other half returned to the oxaloacetate pool distributed on all four carbons. A mathematical description of the process is given in Section 4.3.

The recycling of tracer via the tricarboxylic acid cycle adds radioactivity to the oxaloacetate pool, thus partially cancelling out the effects of the initial dilution caused by the mixing of the different sources of oxaloacetate. The magnitude of the effects of both the metabolic crossover dilution and the subsequent recycling are proportional to the percentage of the molecules in the oxaloacetate pool that arises from the tricarboxylic acid cycle. To correct the

Figure 3-3

The tricarboxylic acid cycle. The carbon skeletons only will be presented in figures 3-4, 5, 7 and 4-1, 2.

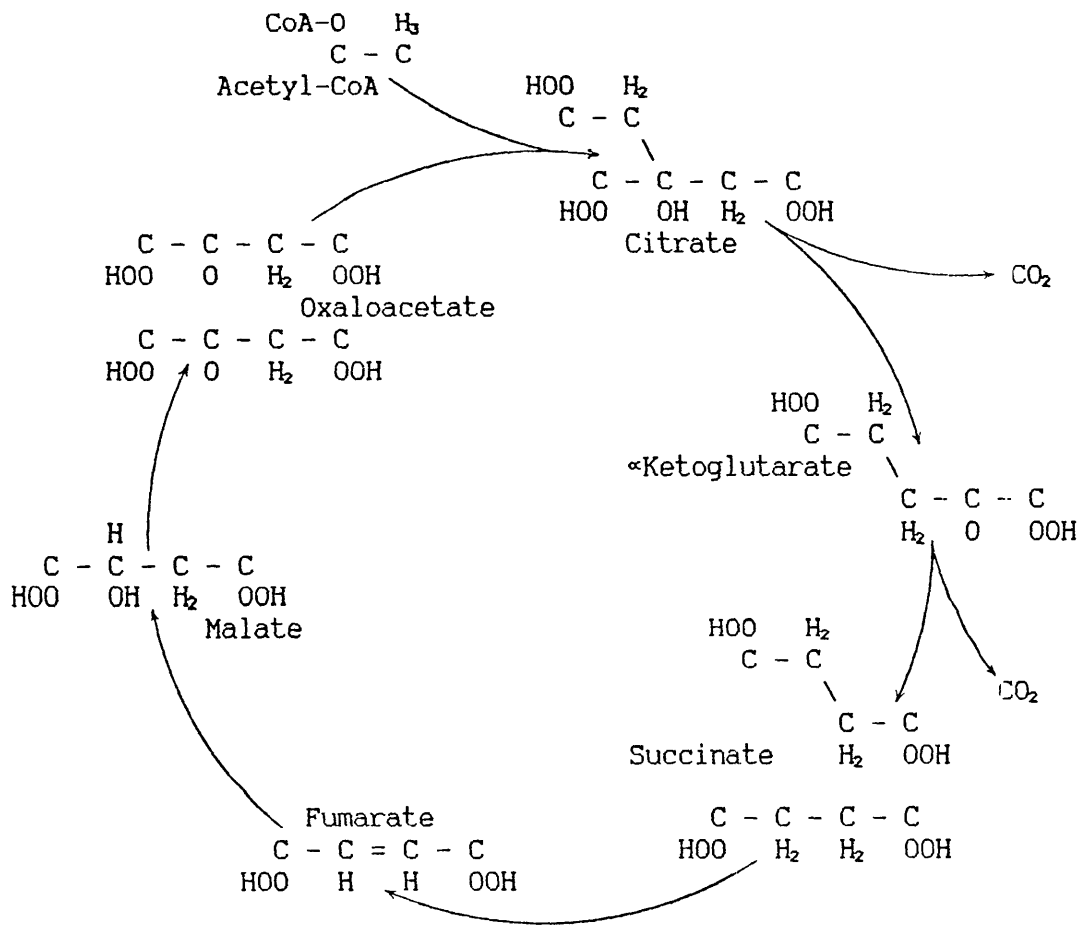


Figure 3-4

The positions of the carbon atoms in the intermediates of the tricarboxylic acid cycle that become labelled when oxaloacetate labelled on the middle carbons first goes round the cycle.

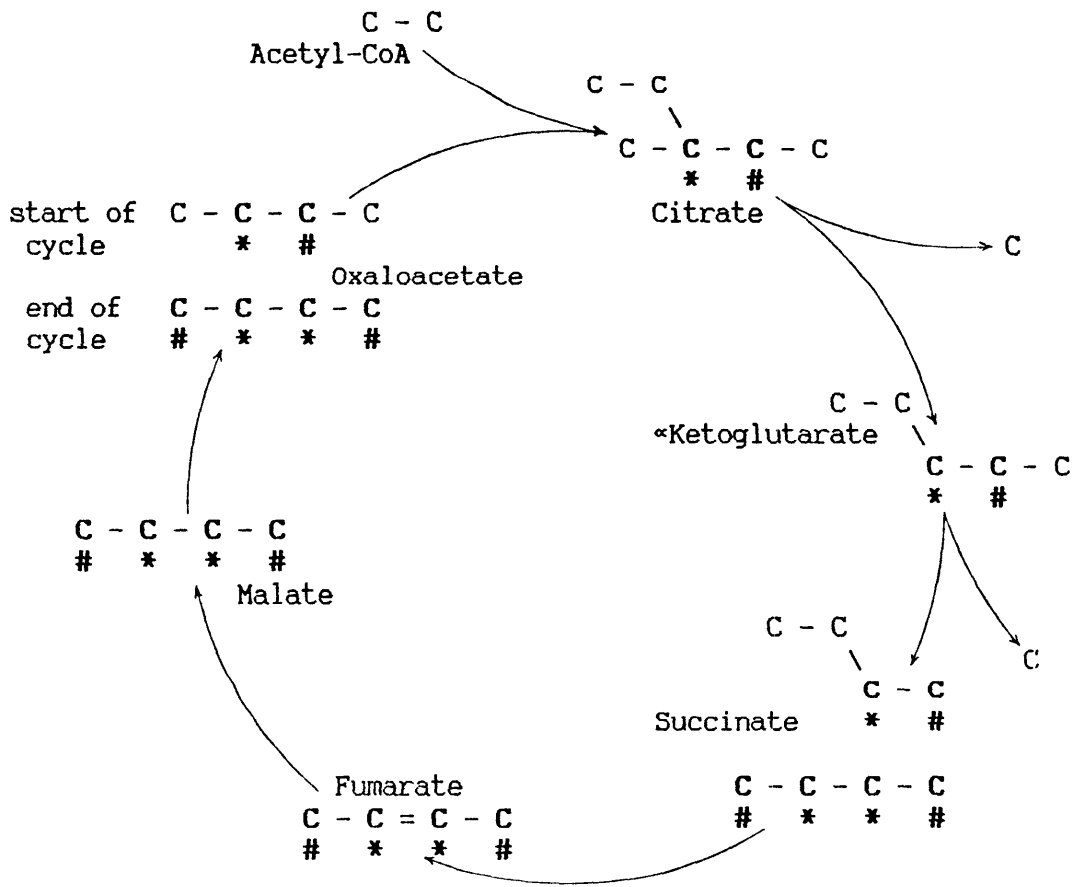
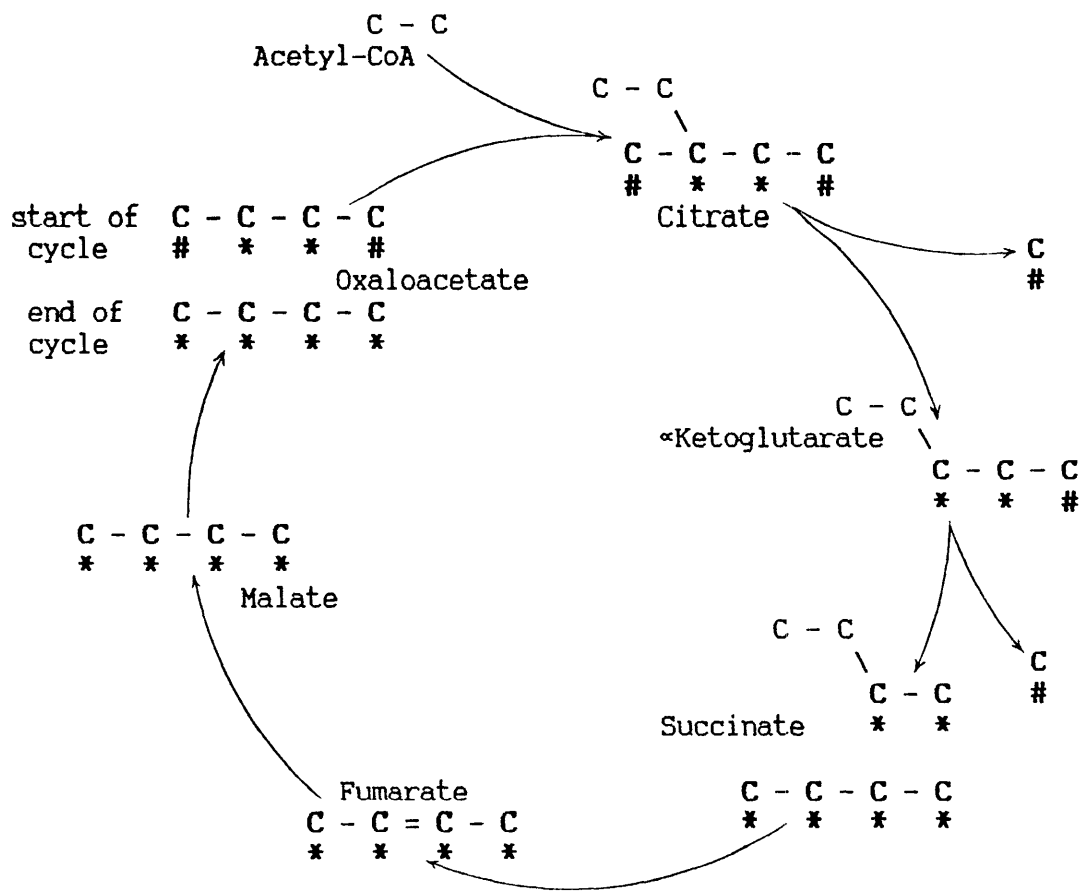


Figure 3-5

The positions of the carbon atoms in the intermediates of the tricarboxylic acid cycle that become labelled when an oxaloacetate that was originally labelled on the middle carbons goes round the cycle for the second time.



transfer quotient for these factors the percentage of the molecules in the oxaloacetate pool that arises from the tricarboxylic acid cycle must be calculated.

### 3.4 PROPIONATE TRACER METABOLISM - [1-<sup>14</sup>C]PROPIONATE

#### 3.4.1 The Positions Of The Carbon Atoms In The Intermediates Which Become Labelled When [1-<sup>14</sup>C]propionate Is Converted Directly To Glucose

The positions of the carbon atoms in the intermediates which become labelled when glucose is synthesized directly from [1-<sup>14</sup>C]propionate are shown in Figure 3-6. The symmetrical compounds, succinate and fumarate, cause the carbon fixed at the carboxylation reaction (propionyl-CoA to methylmalonyl-CoA) to become indistinguishable from the carboxyl carbon of the original propionate molecule. The net effect is that tracer from [1-<sup>14</sup>C]propionate is equally distributed about the carboxyls of the dicarboxylic acids. Because one of the carboxyl carbons is removed on decarboxylation (oxaloacetate to phosphoenolpyruvate), half the tracer from [1-<sup>14</sup>C]propionate is replaced by carbon from CO<sub>2</sub>. Therefore, when considering the proportion of glucose being provided directly by propionate using [1-<sup>14</sup>C]propionate as the tracer, the transfer quotient has to be multiplied by 2 to account for the loss of tracer in the decarboxylation step.

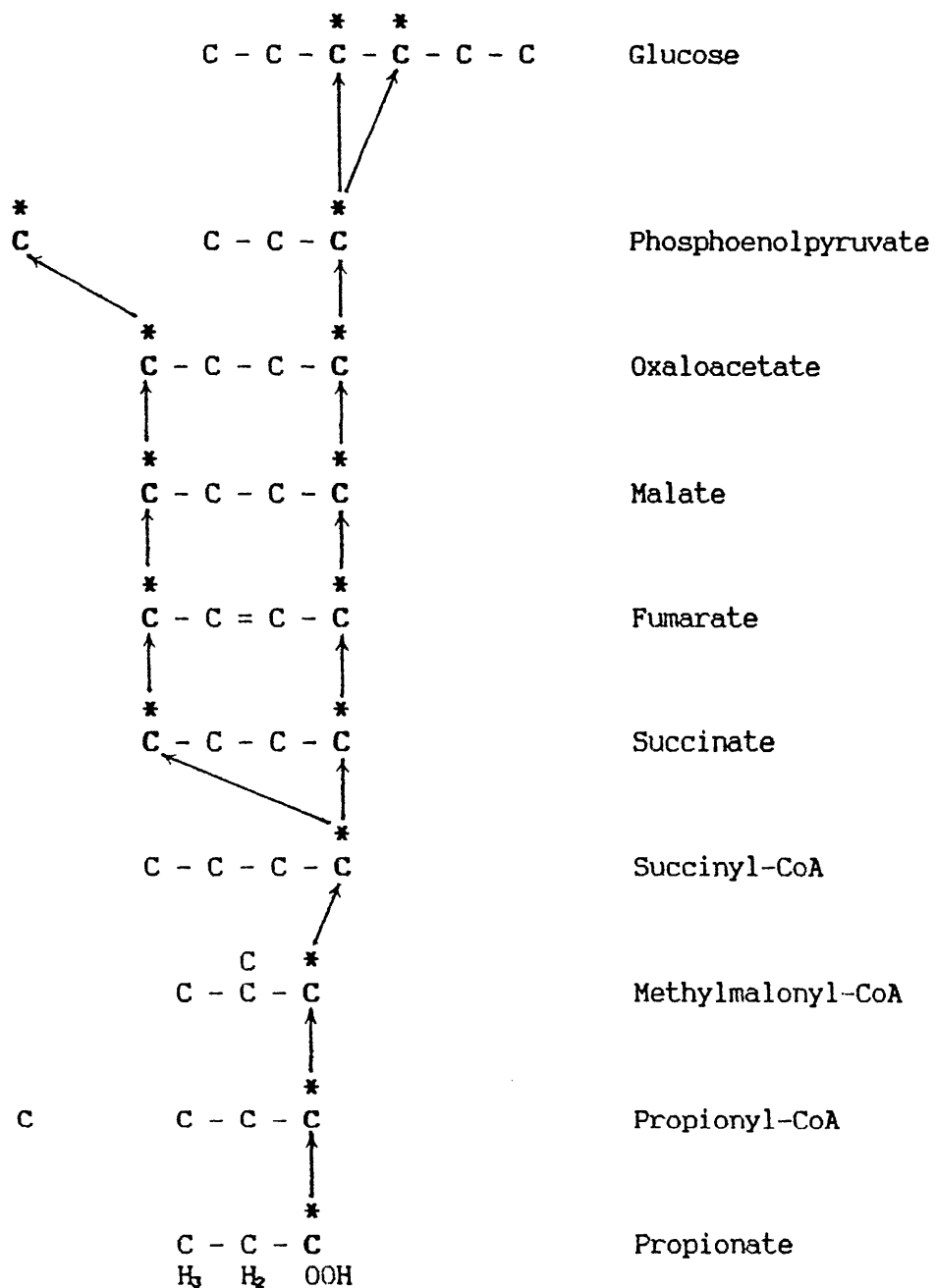
#### 3.4.2 Effect Of Metabolic Crossover On The Interpretation Of The Transfer Quotient

Oxaloacetate derived from propionate mixes with oxaloacetate arising from cycling of the tricarboxylic acid cycle. Thus, the



Figure 3-6

The positions of the carbon atoms in the intermediates which become labelled when [1-<sup>14</sup>C]propionate is converted directly to glucose.



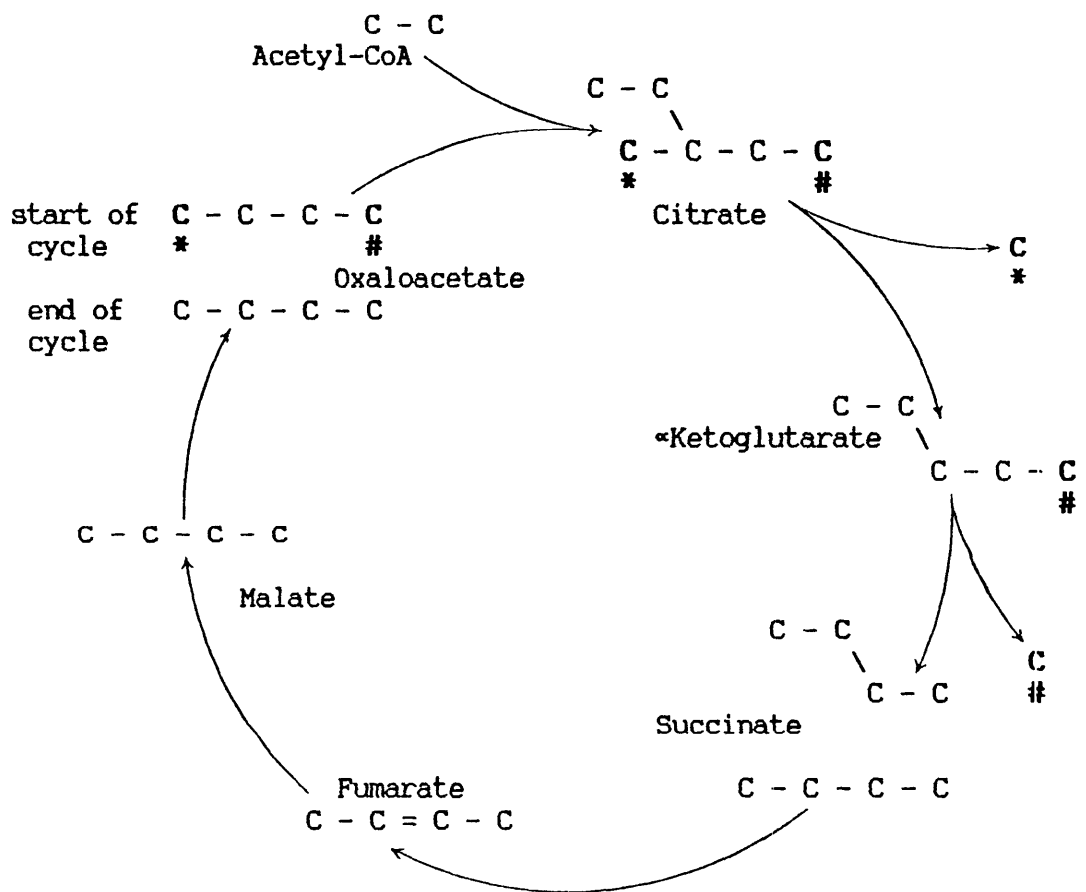
oxaloacetate specific radioactivity is lower than what it would be if this mixing did not occur. Metabolic crossover causes the transfer quotient to underestimate the percentage of glucose provided by propionate.

Tracer from [1-<sup>14</sup>C] propionate labels only the carboxyl positions of oxaloacetate. On one complete turn of the tricarboxylic acid cycle (oxaloacetate to oxaloacetate) both carboxyl carbons of oxaloacetate give rise to CO<sub>2</sub> (Fig 3-7). Therefore, if an oxaloacetate molecule labelled by a [1-<sup>14</sup>C]propionate infusion enters the tricarboxylic acid cycle, no tracer can return to the oxaloacetate pool via the tricarboxylic acid cycle.

The transfer quotient (after correction for the carboxylation/decarboxylation reactions) represents the flow of molecules from propionate direct to glucose (assuming no other pathways of tracer incorporation are operative). To correct the transfer quotient for the effects of metabolic crossover the percentage of the molecules in the oxaloacetate pool from cycling of the tricarboxylic acid cycle needs to be known.

Figure 3-7

The positions of the carbon atoms in the intermediates of the tricarboxylic acid cycle that become labelled when oxaloacetate labelled on the carboxyl carbons goes round the cycle.



## CHAPTER 4

### METHODS OF QUANTIFYING METABOLIC CROSSOVER

#### 4.1 INTRODUCTION

An estimate of the percentage of glucose being provided by propionate can be obtained by measuring the incorporation of tracer from propionate into glucose i.e. the transfer quotient. To correct this percentage to the true contribution of propionate to glucose the effects of metabolic crossover must be accounted for. As the effects of metabolic crossover are proportional to the percentage of the molecules in the oxaloacetate pool that arises from cycling of the tricarboxylic acid cycle, this latter parameter has to be estimated.

In this chapter several methods of estimating the percentage of the molecules in the oxaloacetate pool arising from cycling of the tricarboxylic acid cycle are developed. The first uses the incorporation of the carboxyl carbon of acetyl-CoA into glucose. The second is based on the differential metabolism of [1-<sup>14</sup>C] and [2-<sup>14</sup>C]acetate in the tricarboxylic acid cycle. The third method is similar to the second except that [1-<sup>14</sup>C] and [2-<sup>14</sup>C]propionate are used instead of [1-<sup>14</sup>C] and [2-<sup>14</sup>C]acetate. The fourth method involves the incorporation of <sup>14</sup>CO<sub>2</sub> into glucose. Then, some possible tracer flows not accounted for in the theory used to develop the

formulae are discussed.

#### 4.2 METHOD USING [1-<sup>14</sup>C]ACETATE

On every complete turn of the tricarboxylic acid cycle an acetyl-CoA molecule enters the cycle and two molecules of CO<sub>2</sub> are produced. However, it is not the acetyl-CoA carbon that appears in CO<sub>2</sub> but the carboxyl carbons of the oxaloacetate molecule which condensed with the acetyl-CoA. Therefore, acetate can be used to label the oxaloacetate pool and thus allow an acetyl-CoA to oxaloacetate transfer quotient to be calculated. From this an estimate of the percentage of the molecules in the oxaloacetate pool arising from cycling of the tricarboxylic acid cycle can be obtained.

##### 4.2.1 The Positions Of The Carbon Atoms In The Intermediates Of The Tricarboxylic Acid Cycle Which Become Labelled When [1-<sup>14</sup>C]acetate Enters The Cycle

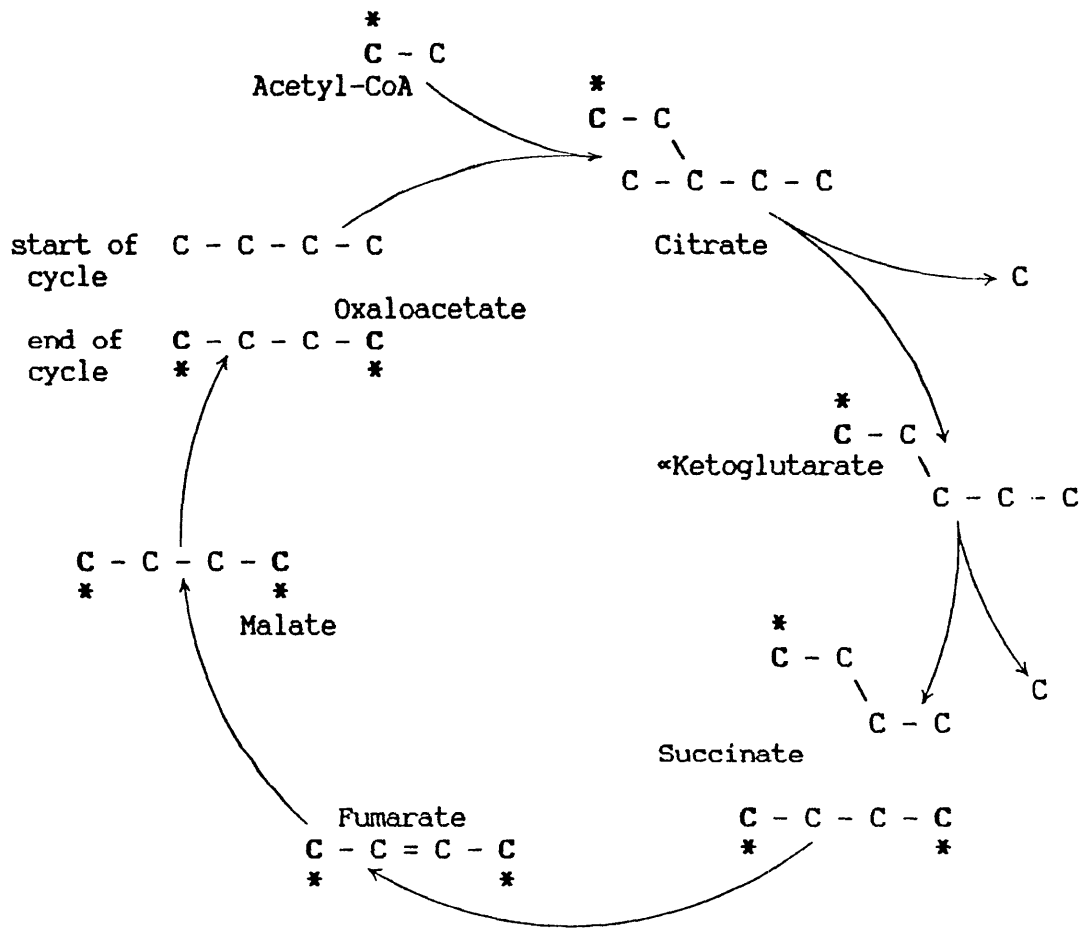
As shown in figure 4-1, [1-<sup>14</sup>C]acetyl-CoA labels both carboxyl carbons of oxaloacetate on the first turn of the cycle. On the subsequent turn of the cycle both carboxyl carbons of oxaloacetate are converted to CO<sub>2</sub> (Figure 3-7). Therefore, tracer from [1-<sup>14</sup>C]acetyl-CoA is not returned to the oxaloacetate pool via continued turning of the tricarboxylic acid cycle.

##### 4.2.2 The Specific Radioactivity Of The Carboxyl Carbons Of Oxaloacetate Labelled By [1-<sup>14</sup>C]acetyl-CoA

The reasoning given in this section is similar to that of Weinman et al. (1957). The specific radioactivity of the carboxyl carbon of oxaloacetate formed from the cycling of the tricarboxylic acid cycle

**Figure 4-1**

The positions of the carbon atoms in the intermediates of the tricarboxylic acid cycle that become labelled when acetyl-CoA labelled on the carboxyl carbon enters the cycle.



only, is related to the specific radioactivity of the carboxyl carbon of the acetyl-CoA entering the cycle by the following equation:

$$\text{OCSR}'' = \text{ASR} \times \frac{1}{2}$$

Where OCSR'' = The specific radioactivity of each carboxyl carbon on the oxaloacetate molecules formed from cycling of the tricarboxylic acid cycle.

ASR = specific activity of the carboxyl carbon of acetyl-CoA entering the tricarboxylic acid cycle.

The factor of  $\frac{1}{2}$  accounts for the randomization of the tracer from acetyl-CoA about both the carboxyls of the symmetrical dicarboxylic acids.

Inflows of oxaloacetate molecules from different sources lower the specific radioactivity of the oxaloacetate carboxyl pool. The extent of this lowering is related to the proportion of the oxaloacetate pool provided by these other sources.

Let NI (net influx) equal the rate of influx to the tricarboxylic acid cycle of unlabelled 4 and 5 carbon compounds relative to the rate of condensation of acetyl-CoA with oxaloacetate, with the latter being defined as unity.

Then,

$$\text{OCSR} = \text{ASR} \times \frac{1}{2} \times \frac{1}{(1+NI)}$$

Where OCSR = the specific radioactivity of each carboxyl carbon of oxaloacetate.

The factor  $(1/(1+NI))$  is the proportion of the oxaloacetate pool provided by cycling of the tricarboxylic acid cycle. It accounts for the dilution of the oxaloacetate pool caused by the net inflows of unlabelled 4 and 5 carbon units.

The above equation can be rearranged to give

$$NI = (ASR / (2 \times OCSR)) - 1$$

If both ASR and OCSR are estimated experimentally, NI and therefore  $(1/(1+NI))$  can also be estimated. This latter value is the fraction of the oxaloacetate pool derived from cycling of the tricarboxylic acid cycle. Since the effects of metabolic crossover are proportional to the fraction of the oxaloacetate pool provided by cycling of the tricarboxylic acid cycle, metabolic crossover can be quantified using this equation.

#### 4.2.3 Estimating OCSR And ASR

The above equation requires an estimate of the specific radioactivity of the appropriate oxaloacetate pool i.e. the pool where oxaloacetate from net glucose precursors mixes with oxaloacetate from the tricarboxylic acid cycle. The specific radioactivity of the oxaloacetate pool can be measured directly, but the assay is inaccurate for several reasons. Firstly, only small quantities of oxaloacetate are present in gluconeogenic tissues at any one time and the amount of tissue that can be taken for analysis is limited. However, the major problem with procedures which measure directly the specific radioactivity of oxaloacetate in the liver is: there are



five different cell types in the liver, and gluconeogenesis occurs in only one of these - the hepatocytes. As hepatocytes constitute only 60 to 65% of the total cell population of the liver (Mullhofer, Muller, Von Stetten and Gruber, 1977a), there could be considerable dilution with oxaloacetate from other cell types during the extraction procedures. Therefore, determining the specific radioactivity of oxaloacetate isolated from a tissue sample need not estimate the parameter required by the above equation. The specific radioactivity of oxaloacetate required by the above equation is that of the oxaloacetate in the compartment of the cell type where gluconeogenesis is occurring. An indirect estimate of this can be obtained by assaying the specific radioactivities of products synthesised from the appropriate oxaloacetate pool. For example, provided all glucose is synthesised from oxaloacetate, the specific radioactivity of glucose carbons 3 or 4 equals the specific radioactivity of the oxaloacetate carboxyl carbons.

To solve the above equation an estimate of the specific radioactivity of the carboxyl carbon of the acetyl-CoA that actually enters the tricarboxylic acid cycle is also required. This is not the same as blood acetate specific radioactivity because there is considerable in situ synthesis of acetyl-CoA from substrates other than acetate. Pethick et al. (1981) reported that acetate uptake by the liver could only account for about 30% of the substrate oxidized as indicated by oxygen uptake. Butyrate and ketone bodies which are extensively metabolised by the liver must also be important precursors of acetyl-CoA. Extracting the acetyl-CoA directly from the liver in order to measure its specific radioactivity presents the problem of dilution by acetyl-CoA from other cell types, possibly other hepatocytes (Sasse, Katz and Jungermann, 1975) and maybe even other

compartments within the cells that are involved in gluconeogenesis.

#### 4.3 METHODS USING [1-<sup>14</sup>C] AND [2-<sup>14</sup>C]ACETATE

Differently labelled species of a compound are affected by the same dilution factors at the molecular level, and thus, in a comparison of product specific radioactivities, these dilution factors will cancel out. Differences in the product specific radioactivities must be due to differences in metabolism of the carbons in the labelled positions.

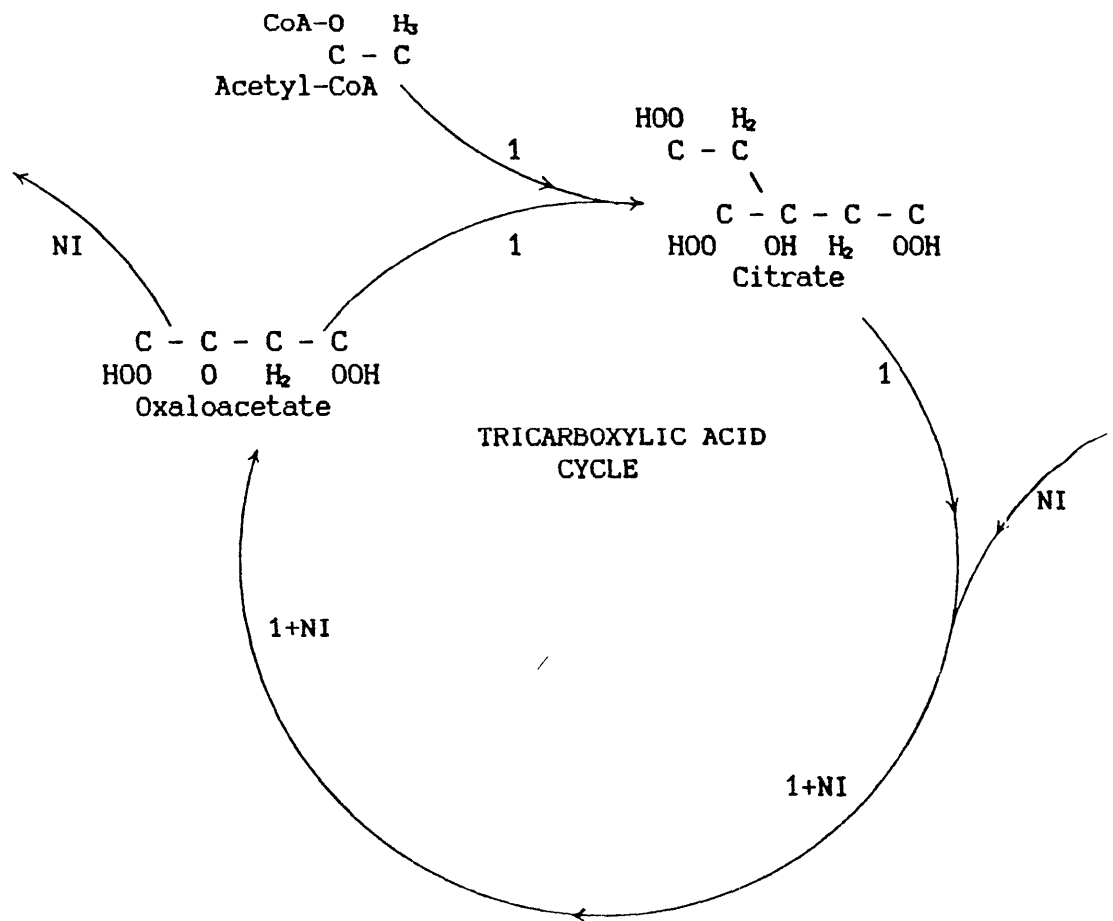
The major difference between the metabolism of tracer from [1-<sup>14</sup>C] and [2-<sup>14</sup>C]acetate is that tracer from [2-<sup>14</sup>C]acetate cycles back to oxaloacetate via the tricarboxylic cycle. Therefore, the ratio of the oxaloacetate specific radioactivities when [1-<sup>14</sup>C] and [2-<sup>14</sup>C]acetates enter the tricarboxylic acid cycle is dependent on the amount of tracer recycling: this, in turn is dependent on the percentage of the molecules in the oxaloacetate pool arising from cycling of the tricarboxylic acid cycle, (the value needed to allow metabolic crossover to be quantified).

##### 4.3.1 The Positions Of The Carbon Atoms In The Intermediates Of The Tricarboxylic Acid Cycle Which Become Labelled When [2-<sup>14</sup>C]acetate Enters The Cycle

An assumption implicit in the following discussion is that steady state conditions apply to the tricarboxylic acid cycle (i.e. the rate of net influx into the cycle must equal the rate of net efflux). This is represented in Figure 4-2.

Figure 4-2

The tricarboxylic acid cycle illustrating conditions of steady state i.e. net influx must equal net efflux (from Weinman et al 1957)



The middle carbons of oxaloacetate are labelled by [2-<sup>14</sup>C]acetate when it first enters the oxaloacetate pool (Figure 4-3). Figures 4-5 to 4-9 show the carbon skeletons of the compounds illustrated in Figure 4-4. These figures illustrate the distribution of tracer in the tricarboxylic acid cycle after a number of complete turns of the cycle under the following conditions:

1. The specific radioactivity of the methyl carbon of the acetyl-CoA entering the cycle = 100.
2. Net input sources of oxaloacetate are providing 60% of the molecules in the oxaloacetate pool.

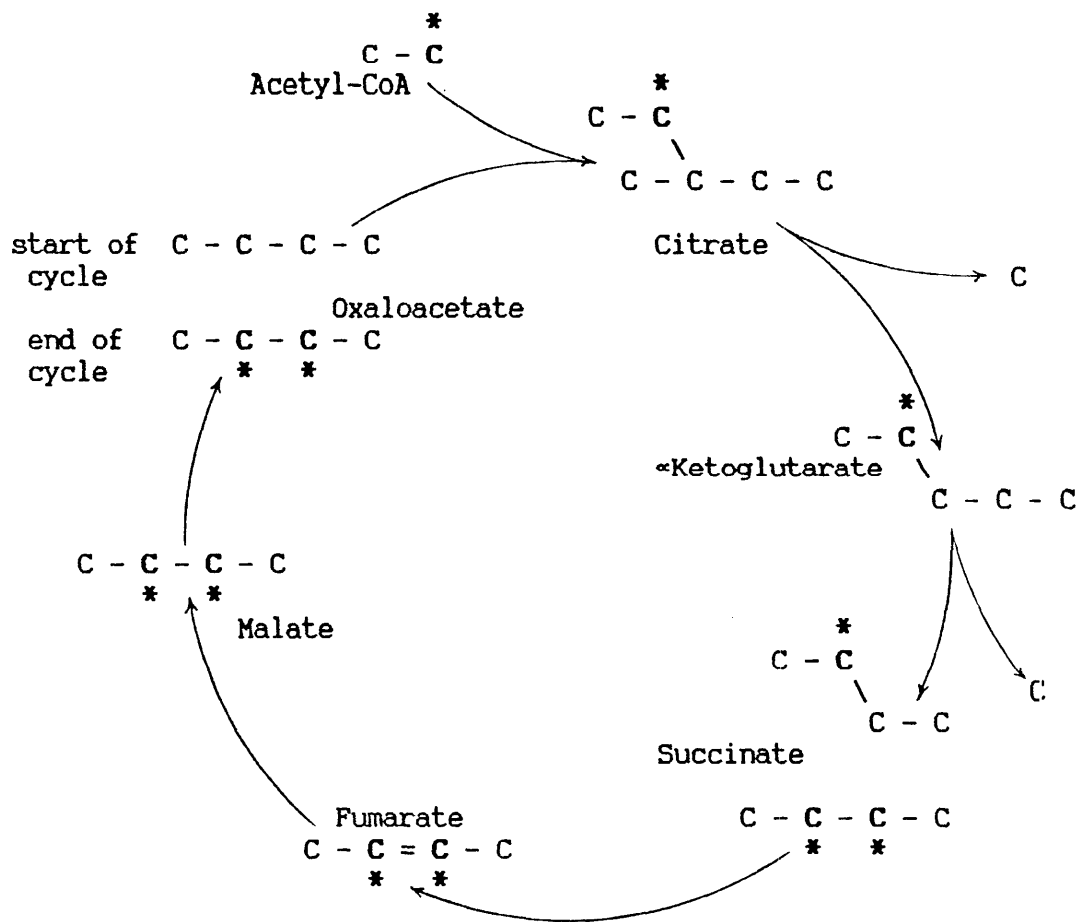
As shown in Figures 4-5 to 4-8, the specific radioactivity of the oxaloacetate carbons increases with each turn of the cycle. Therefore, molecules on their first turn of the cycle (after being labelled) plus those on their second, third and subsequent turns, must all be making a contribution of activity to the specific radioactivity of the carbons of the oxaloacetate pool.

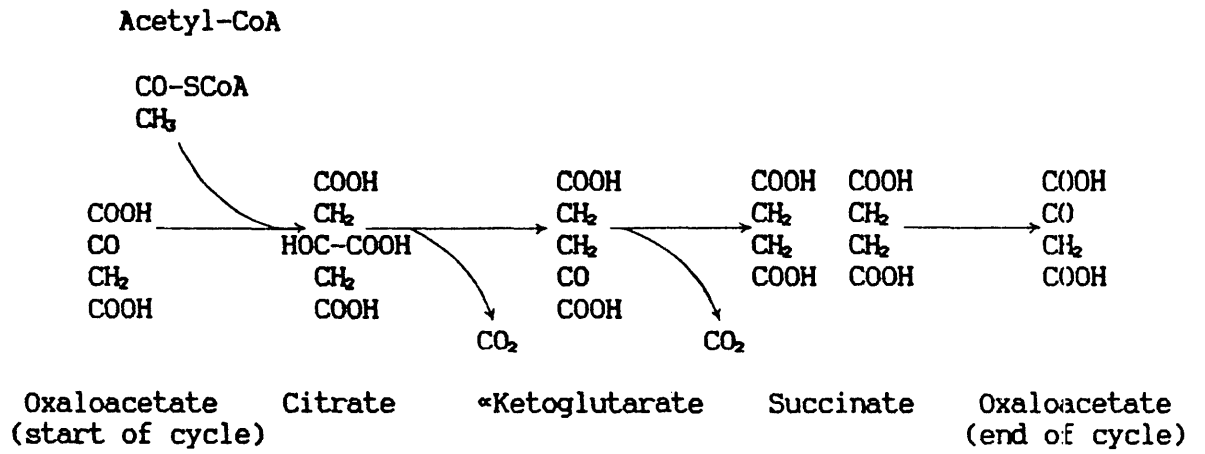
#### 4.3.2 The Specific Radioactivity Of The Middle Carbons Of Oxaloacetate Labelled By [2-<sup>14</sup>C] Acetyl-CoA

Figure 4-9 shows the radioactivity from a single labelled [2-<sup>14</sup>C]acetyl-CoA molecule left in the oxaloacetate pool after several turns of the cycle. The specific radioactivity of the oxaloacetate carbons after any number of turns can be obtained by summing the contributions of radioactivity from molecules on every turn to the required number of turns.

Figure 4-3

The positions of the carbon atoms in the intermediates of the tricarboxylic acid cycle that become labelled when acetyl-CoA labelled on the middle carbons first enters the cycle.





**Figure 4-4**

The intermediates of the tricarboxylic acid cycle. The carbon skeletons only will be presented in figures 4-5 to 4-8.

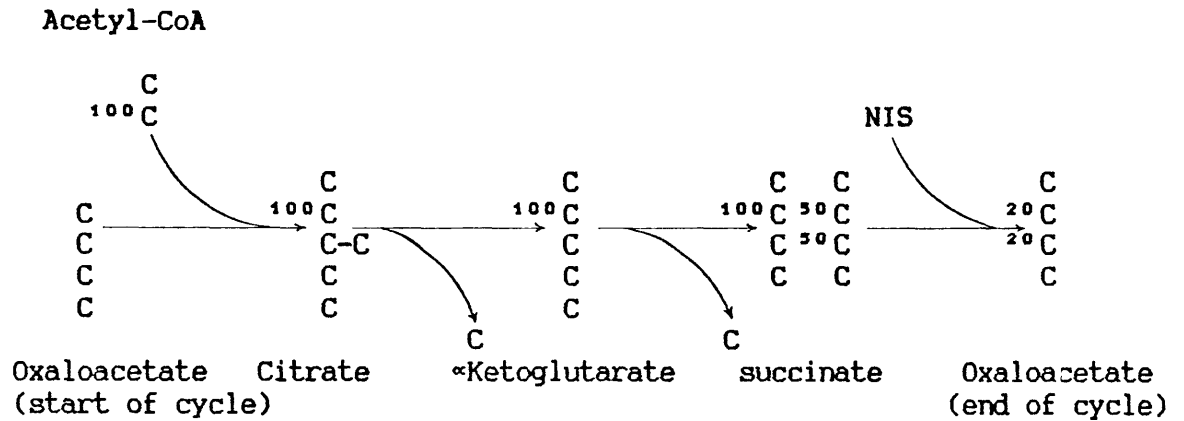


Figure 4-5

The distribution of tracer in intermediates of the tricarboxylic acid cycle on the first turn after labelled acetyl-CoA entered the cycle under the following conditions:

1 The specific radioactivity of the methyl carbon of the acetyl-CoA that entered the cycle was 100.

2 Sixty per cent of the oxaloacetate pool was provided by pathways other than cycling of the tricarboxylic acid cycle (i.e. net input sources = NIS)

The tracer is distributed equally about both the middle carbons of succinate because it is a symmetrical compound. The specific radioactivity of the oxaloacetate pool at the end of the turn is only 20 because of the dilution caused by the net input sources of oxaloacetate. No tracer enters the carboxyl positions of oxaloacetate on the first turn after [2-<sup>14</sup>C]acetyl-CoA molecules enter the cycle.





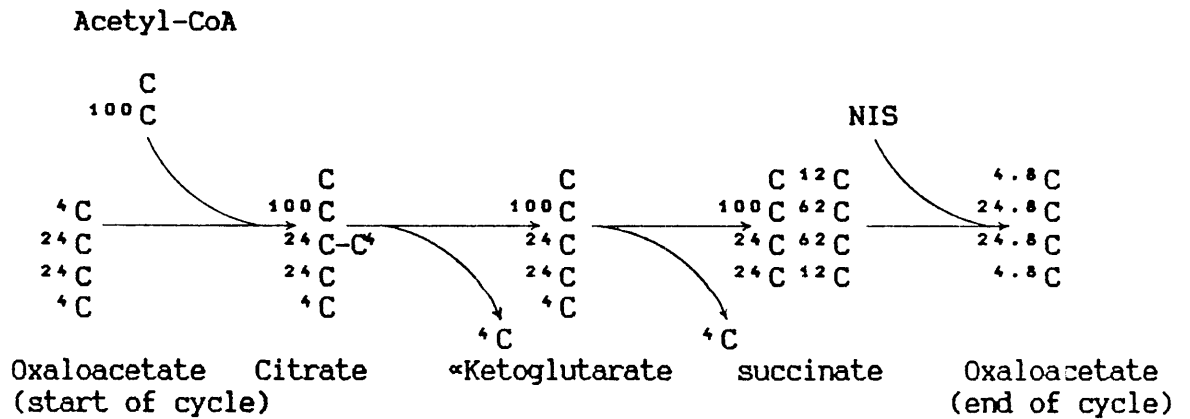


**Figure 4-7**

The distribution of tracer in the intermediates of the tricarboxylic acid cycle when a third labelled acetyl-CoA enters the cycle under the same conditions as figure 4-5.

The tracer again distributes equally about both the middle carbons of succinate. Again, the specific radioactivity of the oxaloacetate at the end of the cycle is greater than that at the start because of label cycling in the cycle. However, the proportional increase in the oxaloacetate specific radioactivity of the third turn over the second is less than the increase of the second over the first.

The carboxyl carbon of succinate derived from the oxaloacetate at the start of the cycle is labelled. This radioactivity becomes distributed equally about both the carboxyls.

The specific radioactivity of the oxaloacetate pool at the end of the turn is again diluted by net input sources of oxaloacetate.

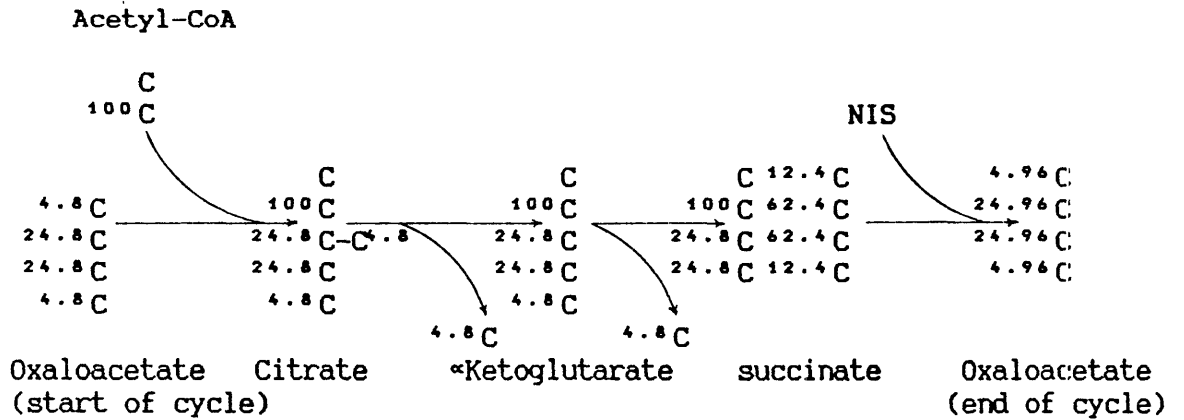


**Figure 4-8**

The distribution of tracer in the intermediates of the tricarboxylic acid cycle when a fourth labelled acetyl-CoA enters the cycle under the same conditions as figure 4-5.

The tracer again distributes equally about both the middle carbons of succinate. Again, the specific radioactivity of the oxaloacetate at the end of the cycle is greater than that at the start because of tracer cycling in the cycle. However, the proportional increase in the oxaloacetate specific radioactivity of the fourth turn over the third is less than the increase of the third over the second. The specific radioactivity of the oxaloacetate pool will approach a limit after several turns.

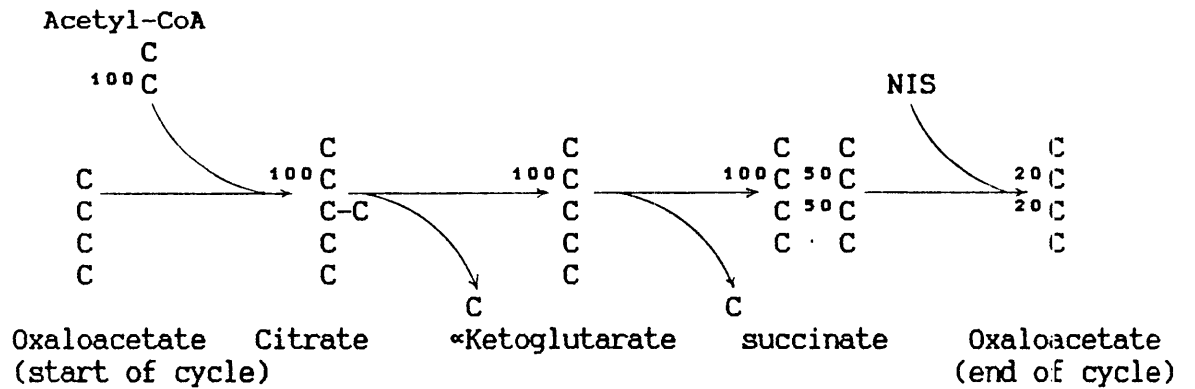
The carboxyl carbon of succinate derived from the oxaloacetate at the start of the cycle is labelled. This radioactivity becomes distributed equally about both the carboxyls.

The specific radioactivity of the oxaloacetate pool at the end of the turn is again diluted by net input sources of oxaloacetate.

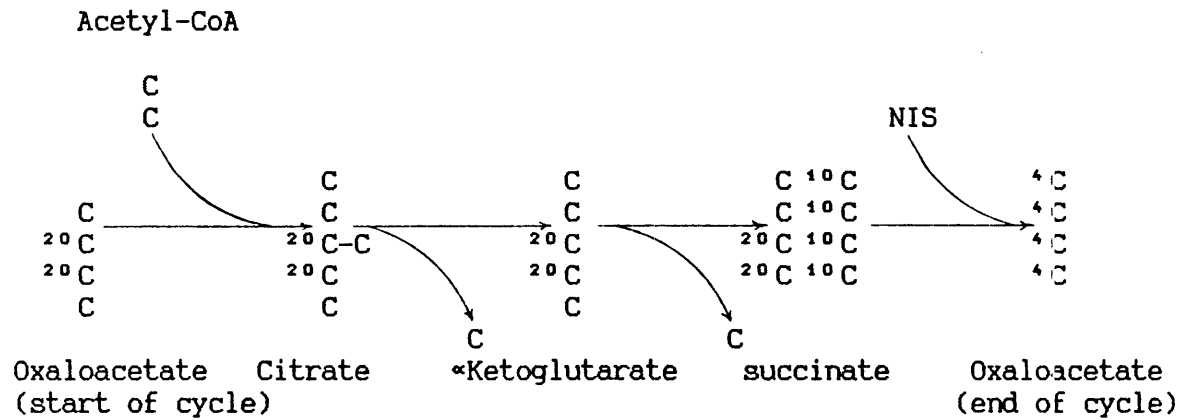
**Figure 4.9**

The distribution of tracer remaining in intermediates of the tricarboxylic acid cycle on various turns after one pulse of labelled acetyl-CoA molecules entered the cycle (under the same conditions as figure 4-5).

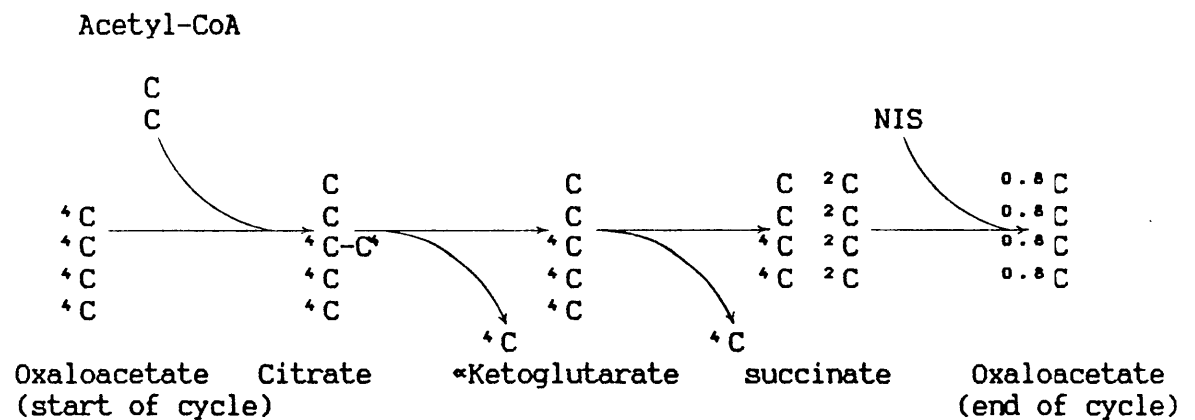
First turn of the cycle



Second turn of the cycle



Third turn of the cycle



The labelling patterns shown in figure 4-9 can be described mathematically by a geometric progression because the contribution of each turn after the first for methyl carbons (after the second for carboxyl carbons) is a constant proportion of the previous turn. Geometric progressions can be summed to infinity and thus the equilibrium specific radioactivities of the oxaloacetate carbons calculated.

On every turn of the cycle, the tracer in the middle carbons of oxaloacetate is affected by equilibration about the middle carbon of succinate (multiply by  $1/2$ ) and by dilution from unlabelled inflows (multiply by  $1/(1+N1)$  - from Section 4.2.2). The specific radioactivity of a methyl carbon of oxaloacetate on the first turn of the cycle after a labelled acetyl-CoA molecule entered it

$$= \text{ASR} \times 1/2 \times 1/(1+N1)$$

The specific radioactivity of a methyl carbon of oxaloacetate on the second turn of the cycle after a labelled acetyl-CoA molecule entered it

$$= \text{starting specific radioactivity} \times 1/2 \times 1/(1+N1)$$

$$= \text{ASR} \times 1/2 \times 1/(1+N1) \times 1/2 \times 1/(1+N1)$$

$$= \text{ASR} \times (1/2 \times 1/(1+N1))^2$$

Similarly, the specific radioactivity of a methyl carbon of oxaloacetate on the third turn of the cycle after a labelled acetyl-CoA molecule entered it

$$= \text{ASR} \times (1/2 \times 1/(1+N1))^3$$

Thus, after n turns, the specific radioactivity remaining on the methyl carbons of oxaloacetate

$$= \text{ASR} \times \left( \frac{1}{2} \times \frac{1}{(1+N1)} \right)^n$$

$$= \text{ASR} \times \left( \frac{1}{(2+2N1)} \right)^n$$

The standard mathematical solution for summing a geometric progression to infinity

$$= \frac{\text{First term of regression}}{1 - \text{the common ratio of terms}}$$

The specific radioactivity of the methyl carbons of oxaloacetate at steady state can be obtained by summing the contributions of radioactivity from each turn of the cycle to infinity.

The specific radioactivity of the methyl carbons of oxaloacetate in steady state

$$\begin{aligned} &= \sum_{n=1}^{\infty} \text{ASR} \times \left( \frac{1}{(2+2N1)} \right)^n \\ &= \left[ \frac{\text{ASR}}{(2+2N1)} \right] / \left[ 1 - \frac{1}{(2+2N1)} \right] \\ &= \text{ASR} / (1+2N1) \end{aligned}$$

#### 4.3.3 The Specific Radioactivity Of The Carboxyl Carbons Of Oxaloacetate Labelled By [2-<sup>14</sup>C]acetyl-CoA

As shown in Figure 4-9 no tracer from [2-<sup>14</sup>C]acetate enters the carboxyl position of oxaloacetate until the second turn of the cycle. The contribution of each turn after this is a constant proportion of the tracer on a methyl carbon of the previous turn. This labelling pattern can also be described mathematically by a geometric progression.

The equilibrium specific radioactivity of the carboxyl carbon

$$\begin{aligned}
 &= \sum_{n=2}^{\infty} ASR \times (1/(2+2NI))^n \\
 &= [ASR/(2+2NI)(2+2NI)] / [1-1/(2+2NI)] \\
 &= ASR/(2+2NI)(1+2NI)
 \end{aligned}$$

#### 4.3.4 The Specific Radioactivity Of The Carboxyl Carbons Of Oxaloacetate Labelled By [1-<sup>14</sup>C]acetyl-CoA

As discussed in section 4.2.2, the equation for the specific radioactivity of the carboxyl carbons of oxaloacetate when [1-<sup>14</sup>C]acetyl-CoA enters the tricarboxylic acid cycle

$$= ASR/(2+2NI)$$

No tracer from [1-<sup>14</sup>C]acetyl-CoA is incorporated into the methyl positions.

#### 4.3.5 Ratios Of Oxaloacetate Specific Radioactivities

The proportional increase in the specific radioactivity of the methyl carbon of oxaloacetate due to recycling of tracer in the tricarboxylic acid cycle above the specific radioactivity due to labelling direct from [2-<sup>14</sup>C]acetate

$$\begin{aligned}
 &= [ASR/(1+2NI)] / [ASR/(2+2NI)] \\
 &= (2+2NI)/(1+2NI)
 \end{aligned}$$

The specific radioactivity of the acetyl-CoA entering the tricarboxylic acid cycle should be the same for both [1-<sup>14</sup>C] and [2-<sup>14</sup>C]acetate at the same rate of tracer infusion. Therefore, the

equation for the proportional increase in the oxaloacetate methyl carbon specific radioactivities ([2-<sup>14</sup>C]acetate infused) over that of the oxaloacetate carboxyl carbon specific radioactivities ([1-<sup>14</sup>C]acetate infused) is the same as above.

With a [2-<sup>14</sup>C]acetate infusion, the specific radioactivity of the carboxyl carbon of oxaloacetate expressed as a proportion of the methyl carbon specific radioactivity

$$= [A^{SR}/(2+2NI)(1+2NI)] / [A^{SR}/(1+2NI)]$$

$$= 1/(2+2NI)$$

The proportional increase in the whole molecule oxaloacetate specific radioactivity ([2-<sup>14</sup>C]acetate infused) over that of the whole molecule oxaloacetate specific radioactivity ([1-<sup>14</sup>C]acetate infused)

$$= [2(A^{SR}/(1+2NI) + A^{SR}/(2+2NI)(1+2NI))] / [2(A^{SR}/(2+2NI))]$$

$$= (3+2NI)/(1+2NI)$$

The common factor in all the above equations is the specific radioactivity of the acetyl-CoA carbon that enters the tricarboxylic acid cycle. In the ratios, the acetyl-CoA specific radioactivities cancel out and leave the ratios defined in terms of NI. If the oxaloacetate specific radioactivities could be estimated, the ratios could be rearranged and solved for NI. This would allow  $1/(1+NI)$  (the percentage of the molecules in the oxaloacetate pool arising from cycling of the tricarboxylic acid cycle) to be calculated.

#### 4.3.6 Ratios Of Metabolites Synthesised From Oxaloacetate

The specific radioactivities of the carbons of oxaloacetate can be estimated indirectly by measuring the specific radioactivity of metabolites synthesised from oxaloacetate. It is not necessary to have all the product synthesised from oxaloacetate because any dilution will affect both sides of the ratios equally and thus cancel out. If, in ratios of these products synthesised from oxaloacetate, the specific radioactivity of the acetyl-CoA that enters the cycle cancels out, the ratios can be solved for NI.

Weinman et al. (1957) defined a CO<sub>2</sub> ratio and a glucose ratio. They also defined a glucose labelling ratio, but because this requires analysis of each carbon of the glucose molecule, it was not used in this thesis.

##### 4.3.6.1 CO<sub>2</sub> Ratio -

This ratio is defined as (<sup>14</sup>CO<sub>2</sub> derived from [1-<sup>14</sup>C]acetate) divided by (<sup>14</sup>CO<sub>2</sub> derived from [2-<sup>14</sup>C]acetate). Since the equilibrium specific radioactivity of the carboxyl carbons of oxaloacetate determines directly the amount of <sup>14</sup>CO<sub>2</sub> expired, the above ratio can be written as:

$$\frac{\text{specific radioactivity of the carboxyl carbon of oxaloacetate derived from [1-}^{14}\text{C]acetate}}{\text{specific radioactivity of the carboxyl carbon of oxaloacetate derived from [2-}^{14}\text{C]acetate}}$$

$$= \left[ \frac{A^{SR}}{(2+2NI)} \right] / \left[ \frac{A^{SR}}{(2+2NI)(1+2NI)} \right]$$

$$= 1 + 2NI$$



#### 4.3.6.2 Glucose Ratio -

The glucose ratio is defined as: ( $^{14}\text{C}$  incorporated into glucose from  $[2\text{-}^{14}\text{C}]\text{acetate}$ ) divided by ( $^{14}\text{C}$  incorporated into glucose from  $[1\text{-}^{14}\text{C}]\text{acetate}$ ), by way of the pathway: acetate, tricarboxylic acid cycle, oxaloacetate, pyruvate, glucose.

Therefore, in terms of the specific radioactivity of oxaloacetate carbons, the glucose ratio

$$\begin{aligned}
 &= \frac{2 \times \left[ \begin{array}{c} \text{specific radioactivity of} \\ \text{the middle carbons of} \\ \text{oxaloacetate} \\ \text{([2-}^{14}\text{C]acetate infused)} \end{array} \right] + \left[ \begin{array}{c} \text{specific radioactivity of} \\ \text{the carboxyl carbons of} \\ \text{oxaloacetate} \\ \text{([2-}^{14}\text{C]acetate infused)} \end{array} \right]}{\text{specific radioactivity of carboxyl carbons of oxaloacetate} \\
 &\quad \text{derived from [1-}^{14}\text{C]acetate}} \\
 &= [2(\text{ASR}/(1+2\text{NI})) + (\text{ASR}/(2+2\text{NI})(1+2\text{NI}))] / [\text{ASR}/(2+2\text{NI})] \\
 &= 5+4\text{NI}/(1+2\text{NI})
 \end{aligned}$$

#### 4.3.7 Conclusion

Because the glucose and bicarbonate specific radioactivities can be measured, it is possible to solve the above ratios for NI and thus  $1/(1+\text{NI})$ . This allows the effects of metabolic crossover to be quantified.

#### 4.4 METHOD USING $[1\text{-}^{14}\text{C}]$ AND $[2\text{-}^{14}\text{C}]\text{PROPIONATE}$

Oxaloacetate is labelled by  $[1\text{-}^{14}\text{C}]$  and  $[2\text{-}^{14}\text{C}]\text{propionate}$  in the same positions as  $[1\text{-}^{14}\text{C}]$  and  $[2\text{-}^{14}\text{C}]\text{acetate}$  respectively. Therefore, the reasoning used to develop equations for the percentage of the molecules in the oxaloacetate pool provided by cycling of the tricarboxylic acid cycle using the labelling patterns of acetate can also be used to develop similar equations using labelled propionate.

#### 4.4.1 The Specific Radioactivity Of The Carboxyl Carbons Of Oxaloacetate Labelled By [1-<sup>14</sup>C]propionate

Using the same reasoning as for [1-<sup>14</sup>C]acetate (Section 4.2.2), the equation relating the specific radioactivity of the oxaloacetate carboxyls to the specific radioactivity of the carboxyl carbon of propionate is:

$$\text{OCSR} = \text{PSR} \times \frac{1}{2} \times \frac{1}{(1+\text{NPS})}$$

where OCSR = specific radioactivity of the oxaloacetate carboxyl carbons.

PSR = specific radioactivity of the carboxyl carbon of the succinyl-CoA derived from propionate that enters the cycle (equals the specific radioactivity of the carboxyl carbon of the propionate from which it was derived).

NPS = rate of formation of oxaloacetate from precursors other than propionate relative to the rate of formation from propionate, which is taken as unity.

The factor of  $\frac{1}{2}$  accounts for the randomization of tracer about the carboxyls of oxaloacetate due to the transfer through the symmetrical compounds.

The factor  $(\frac{1}{(1+\text{NPS})})$  is the proportion of the oxaloacetate pool provided by propionate and accounts for the dilution of the oxaloacetate pool derived from propionate by oxaloacetate derived from other sources.

The equation can be rearranged to give

$$NPS = (P^{SR} / (2 \times OCSR)) - 1$$

Unlike acetate, the in situ synthesis of propionate in the liver should be negligible when compared with the amounts absorbed from the digestive tract in the absorptive state. If it is assumed that the rumen propionate carboxyl specific radioactivity is an appropriate value to use in the above equation, the percentage of the molecules in the oxaloacetate pool arising from propionate can be calculated.

#### 4.4.2 The Specific Radioactivity Of The Carbons Of Oxaloacetate Labelled By [2-<sup>14</sup>C]propionate

##### 4.4.2.1 Middle Carbons Of Oxaloacetate -

The distribution of tracer in oxaloacetate when [2-<sup>14</sup>C]propionate first enters the oxaloacetate pool is illustrated in figure 4-10. In the example it is assumed that 40% of the oxaloacetate pool arose from propionate, 20% from other net input sources and 40% from the tricarboxylic acid cycle. The distributions of tracer when second and third labelled propionate molecules enter the oxaloacetate pool are illustrated in figures 4-11 and 4-12. Because the oxaloacetate pool becomes labelled, some labelled oxaloacetate molecules enter the tricarboxylic acid cycle and thus tracer cycles back to the oxaloacetate pool. As illustrated in Figures 4-11 and 4-12, the specific radioactivities of the carbons of oxaloacetate are increased by this recycling.

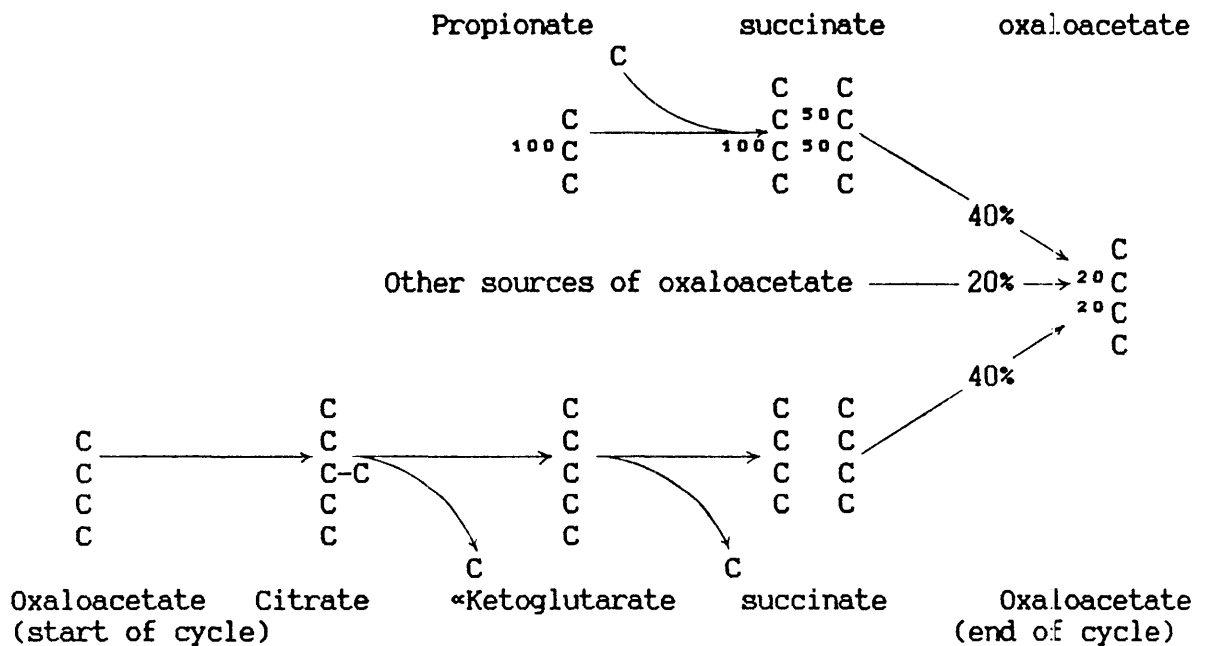


Figure 4-10

The distribution of tracer in Oxaloacetate when one molecule derived from labelled propionate enters the tricarboxylic acid cycle under the following conditions:

- 1 The specific radioactivity of the middle carbon of propionate was 100.
- 2 40% of the oxaloacetate pool was provided by cycling of the tricarboxylic acid cycle
- 3 40% of the oxaloacetate pool was provided by molecules derived from propionate
- 4 20% of the oxaloacetate pool was provided by molecules derived from other net sources.

The tracer is distributed equally about both the middle carbons of succinate because it is a symmetrical compound. The specific radioactivity of the oxaloacetate pool is only 20 because of the dilution caused by the other sources of oxaloacetate. No tracer enters the carboxyl positions of oxaloacetate when molecules labelled by  $[2-^{14}\text{C}]$ propionate first enter the oxaloacetate pool.

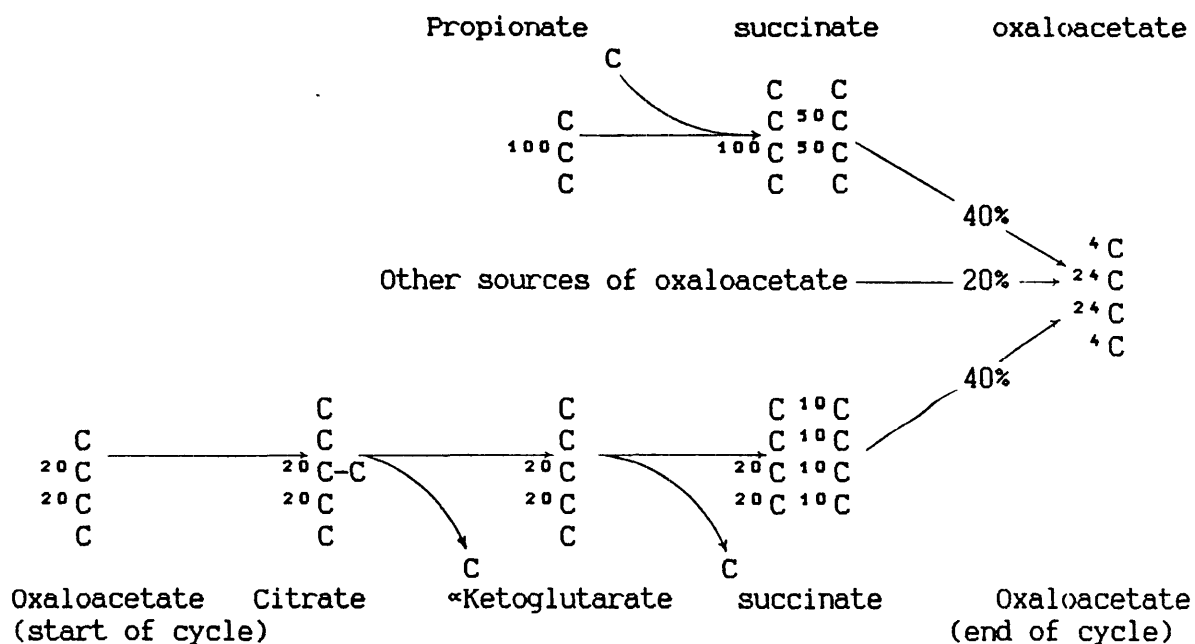


Figure 4-11

The distribution of tracer in oxaloacetate when a second molecule derived from labelled propionate enters the tricarboxylic acid cycle under the same conditions as in figure 4-10.

Because the oxaloacetate molecules arising from the tricarboxylic cycle are labelled, the specific radioactivity of the oxaloacetate pool at the end of the cycle will increase. This cycling of tracer also causes the carboxyl carbons to become labelled.

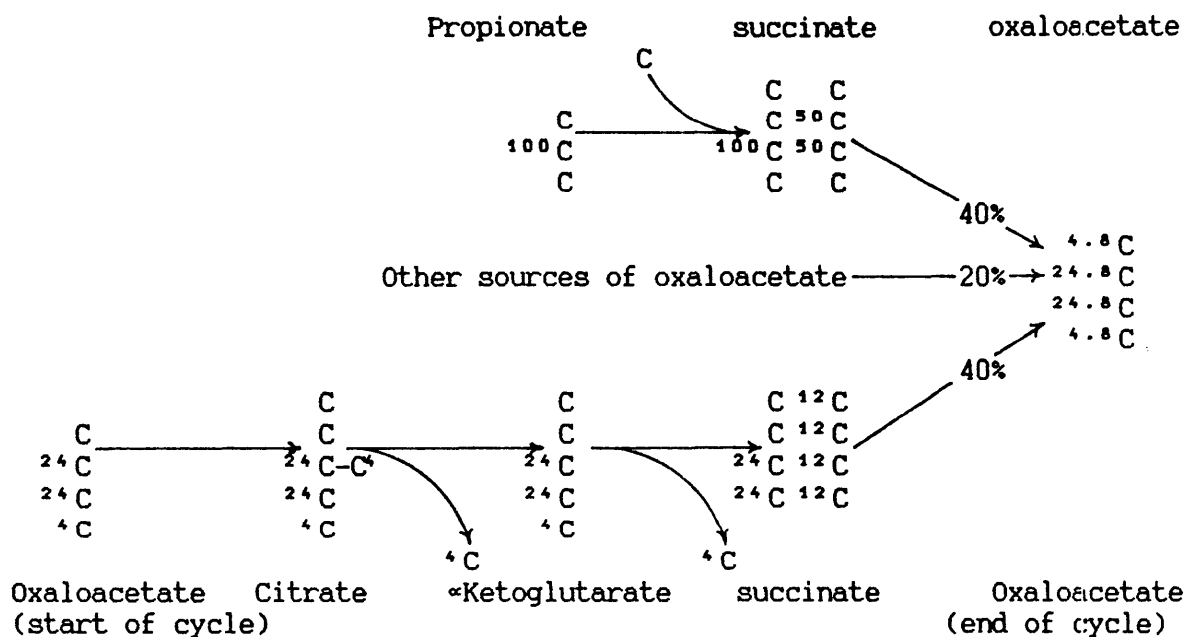


Figure 4-12

The distribution of tracer in oxaloacetate when a third molecule derived from labelled propionate enters the tricarboxylic acid cycle under the same conditions as in figure 4-10.

Again the specific radioactivity of the oxaloacetate pool increased due to tracer cycling in the cycle. However, the increase in specific radioactivity due to the second turn of the cycle is not as great as that due to the first turn. As in the case where  $[2\text{-}^{14}\text{C}]\text{acetate}$  was entering the cycle, the specific radioactivity of the oxaloacetate pool will approach a limit after several turns of the cycle.

Figure 4-13 illustrates the distribution of tracer remaining in the tricarboxylic acid cycle intermediates for 2 turns of the cycle after one oxaloacetate molecule derived from [2-<sup>14</sup>C]propionate enters in the tricarboxylic acid cycle. The reasoning and mathematical equations that described cycling of tracer from [2-<sup>14</sup>C]acetate in the tricarboxylic acid cycle will also describe the cycling of tracer from [2-<sup>14</sup>C]propionate in the tricarboxylic acid cycle.

When molecules derived from propionate first enter the oxaloacetate pool, the specific radioactivity of the carbons have been affected by equilibration of tracer caused by the symmetrical compounds and dilution by molecules not derived from propionate (same as for [1-<sup>14</sup>C]propionate). Therefore, the specific radioactivity of the methyl carbons of oxaloacetate when propionate first enters the tricarboxylic acid cycle

$$= \text{PSR} \times \frac{1}{2} \times \frac{1}{(1 + \text{NPS})}$$

$$= \text{PSR} \times \frac{1}{(2 + 2\text{NPS})}$$

In this case PSR refers to the middle carbon of propionate, not the carboxyl carbon.

As with [2-<sup>14</sup>C]acetate the tracer returned to oxaloacetate by a turn of the tricarboxylic acid cycle is affected by the equilibration of tracer about the symmetrical compounds (multiply by  $\frac{1}{2}$ ) and the proportion of the molecules in the oxaloacetate pool that arose from pathways other than cycling of the tricarboxylic acid cycle (multiply by  $\frac{1}{(1 + \text{NPS})}$ ). Therefore, the tracer returned to oxaloacetate by the first turn of the tricarboxylic acid cycle





$$= \text{starting specific radioactivity} \times \frac{1}{2} \times \frac{1}{(1+N1)}$$

$$= \text{starting specific radioactivity} \times \frac{1}{(2+2N1)}$$

$$(\text{Starting specific radioactivity} = \text{PSR} \times \frac{1}{(2+2NPS)})$$

$$= \text{PSR} \times \frac{1}{(2+2NPS)} \times \frac{1}{(2+2N1)}$$

The tracer returned by the second turn of the cycle

$$= \text{PSR} \times \frac{1}{(2+2NPS)} \times \frac{1}{(2+2N1)} \times \frac{1}{(2+2N1)}$$

$$= \text{PSR} \times \frac{1}{(2+2NPS)} \times \left(\frac{1}{(2+2N1)}\right)^2$$

The tracer returned by the third turn of the cycle

$$= \text{PSR} \times \frac{1}{(2+2NPS)} \times \left(\frac{1}{(2+2N1)}\right)^3$$

Therefore, the tracer returned by the  $n^{\text{th}}$  turn of the cycle

$$= \text{PSR} \times \frac{1}{(2+2NPS)} \times \left(\frac{1}{(2+2N1)}\right)^n$$

The steady state specific radioactivity of the methyl carbon of oxaloacetate when  $[2-^{14}\text{C}]$ propionate is infused is the sum of the radioactivity in oxaloacetate directly from propionate, plus the contribution from tracer cycling in the tricarboxylic acid cycle. Therefore, the steady state specific radioactivity of the methyl carbon of oxaloacetate

$$= \text{PSR} / (2+2NPS) + \sum_{n=1}^{\infty} (\text{PSR} / (2+2NPS)) \times \left(\frac{1}{(2+2N1)}\right)^n$$

$$= \text{PSR} / (2+2NPS) + [\text{PSR} / (2+2NPS)(2+2N1)] / [1 - \frac{1}{(2+2N1)}]$$

$$= [\text{PSR} \times (2+2N1)] / [(2+2NPS)(1+2N1)]$$

#### 4.4.2.2 Carboxyl Carbons Of Oxaloacetate -

As shown in Figure 4-13 no tracer enters the carboxyl positions of oxaloacetate directly from [2-<sup>14</sup>C]propionate but enters from cycling in the tricarboxylic acid cycle. The tracer entering the carboxyl positions comes from one of the middle carbons of the previous turn and is equal to the amount of tracer returned to the central positions on each turn.

Therefore, the steady state specific radioactivity of the carboxyl of oxaloacetate when [2-<sup>14</sup>C]propionate is infused

$$\begin{aligned}
 &= \sum_{n=1}^{\infty} P^{SR} / (2 + 2NP^S) \times (1 / (2 + 2N_1))^n \\
 &= [P^{SR} / (2 + 2NP^S)(2 + 2N_1)] / [1 - 1 / (2 + 2N_1)] \\
 &= P^{SR} / (2 + 2NP^S)(1 + 2N_1)
 \end{aligned}$$

#### 4.4.3 Ratios Of Oxaloacetate Specific Radioactivities

The major difference between the metabolism of tracer from [1-<sup>14</sup>C] and [2-<sup>14</sup>C]propionate is the recycling of tracer from [2-<sup>14</sup>C]propionate in the tricarboxylic acid cycle. Therefore, a ratio of the oxaloacetate specific radioactivities when [1-<sup>14</sup>C] and [2-<sup>14</sup>C]propionate are infused, should cancel the effects of the initial direct labelling of the oxaloacetate pool by propionate and leave the ratio proportional to the amount of tracer cycling in the tricarboxylic acid cycle. The rate of recycling is proportional to the percentage of the molecules in the oxaloacetate pool coming from cycling of the tricarboxylic acid cycle. This is similar reasoning to that used in developing ratios using [1-<sup>14</sup>C] and [2-<sup>14</sup>C]acetate (section 4.4.3) and similar ratios can be defined.

The proportional increase in the specific radioactivity of the middle carbon of oxaloacetate due to equilibrium of tracer in the tricarboxylic acid cycle over the specific radioactivity due to labelling direct from [2-<sup>14</sup>C]propionate

$$= \frac{[P^{SR}(2+2NI)] / [(2+2NPS)(1+2NI)]}{[P^{SR} / (2+2NPS)]}$$

$$= \frac{(2+2NI)}{(1+2NI)}$$

With the same propionate specific radioactivities the equation for the proportional increase in the oxaloacetate middle carbon specific radioactivity ([2-<sup>14</sup>C]propionate infused) above that of oxaloacetate carboxyl carbon specific radioactivity ([1-<sup>14</sup>C]propionate infused) is the same as the above.

With a [2-<sup>14</sup>C]propionate infusion, the specific radioactivity of the carboxyl carbon of oxaloacetate expressed as a proportion of the methyl carbon of oxaloacetate

$$= \frac{[P^{SR} / (2+2NPS)(1+2NI)]}{[P^{SR}(2+2NI) / (2+2NPS)(1+2NI)]}$$

$$= \frac{1}{(2+2NI)}$$

The proportional increase in the whole molecule oxaloacetate specific radioactivity ([2-<sup>14</sup>C]propionate infused) over that of the whole molecule oxaloacetate specific radioactivity ([1-<sup>14</sup>C]propionate infused)

$$= 2 \frac{[P^{SR} / (2+2NPS)(1+2NI) + P^{SR}(2+2NI) / (2+2NPS)(1+2NI)]}{2[P^{SR} / (2+2NPS)]}$$

$$= \frac{3+2NI}{(1+2NI)}$$

#### 4.4.4 Ratios Of Metabolites Synthesised From Oxaloacetate

4.4.4.1 CO<sub>2</sub> Ratio - The ratio is defined as CO<sub>2</sub> derived from [1-<sup>14</sup>C]propionate divided by CO<sub>2</sub> derived from [2-<sup>14</sup>C]propionate. This is equivalent to

$$\frac{\text{specific radioactivity of the carboxyl carbon of oxaloacetate derived from [1-}^{14}\text{C]propionate}}{\text{specific radioactivity of the carboxyl carbon of oxaloacetate derived from [2-}^{14}\text{C]propionate}}$$

$$= \left[ \frac{P^{SR}}{(2+2NPS)} \right] / \left[ \frac{P^{SR}}{(2+2NPS)(1+2NI)} \right]$$

$$= 1 + 2NI$$

This equation can be solved to calculate a value of NI. Thus the proportion of the oxaloacetate pool coming from cycling of the tricarboxylic acid cycle ( $1/(1+NI)$ ) can also be calculated.

4.4.4.2 Glucose Ratio - The glucose ratio is defined as: <sup>14</sup>C incorporated into glucose from [2-<sup>14</sup>C]propionate divided by <sup>14</sup>C incorporated into glucose from [1-<sup>14</sup>C]propionate. This is equivalent to

$$2 \times \frac{\left[ \begin{array}{c} \text{specific radioactivity of} \\ \text{the middle carbons of} \\ \text{oxaloacetate} \\ \text{([2-}^{14}\text{C]propionate infused)} \end{array} \right] + \left[ \begin{array}{c} \text{specific radioactivity of} \\ \text{the carboxyl carbons of} \\ \text{oxaloacetate} \\ \text{([2-}^{14}\text{C]propionate infused)} \end{array} \right]}{\text{specific radioactivity of carboxyl carbons of oxaloacetate derived from [1-}^{14}\text{C]propionate}}$$

$$= \frac{2 \left( \frac{P^{SR}(2+2NI)}{(2+2NPS)(1+2NI)} \right) + \frac{P^{SR}}{(2+2NPS)(1+2NI)}}{\left[ \frac{P^{SR}}{(2+2NPS)} \right]}$$

$$= \frac{5+4NI}{(1+2NI)}$$

The equation can be solved for NI and the proportion of the molecules in the oxaloacetate pool coming from cycling of the tricarboxylic acid cycle ( $1/(1+NI)$ ) can also be calculated.

#### 4.4.5 Conclusion

All the above ratios developed using [1-<sup>14</sup>C] and [2-<sup>14</sup>C]propionate are exactly the same as those defined using [1-<sup>14</sup>C] and [2-<sup>14</sup>C]acetate. This is as expected because, for both acids, the initial labelling of the oxaloacetate pool cancels, leaving the ratio proportional to the amount of recycling. Any compound that has labelled species that will label oxaloacetate in the same manner as [1-<sup>14</sup>C] and [2-<sup>14</sup>C]acetate will have the initial labelling of the oxaloacetate pool cancel out in ratios similar to the above.

If only one tissue is producing <sup>14</sup>CO<sub>2</sub> from [1-<sup>14</sup>C] and [2-<sup>14</sup>C]acetate or propionate, then the CO<sub>2</sub> ratio using blood bicarbonate values will be the same as the CO<sub>2</sub> ratio of that tissue. The specific radioactivities of CO<sub>2</sub> in blood will be less than that in the tissue due to dilution with CO<sub>2</sub> produced in other tissues but, the effect of this will cancel out in the ratio. However, if <sup>14</sup>CO<sub>2</sub> is produced in several tissues of the body, then the value of the CO<sub>2</sub> ratio using blood bicarbonate specific radioactivities need not be the same as the value of the CO<sub>2</sub> ratio of the individual tissues. As the CO<sub>2</sub> ratio is calculated in order to estimate the effects of metabolic crossover on the propionate to glucose transfer quotient, the CO<sub>2</sub> ratio required is that of the gluconeogenic tissues; most of which is in the liver. Acetate is metabolized in many tissues of the body, therefore using blood bicarbonate specific radioactivities to solve the CO<sub>2</sub> ratio will not reflect the value of the CO<sub>2</sub> ratio of the gluconeogenic tissues, but, the average CO<sub>2</sub> ratio of those tissues that oxidize acetate.

As almost all propionate is extracted on its first pass through the liver (Annison et al., 1957), very little propionate produced in the rumen reaches tissues other than those in the liver. In the liver propionate is used extensively as a glucose precursor. Therefore, the value of the CO<sub>2</sub> ratio using blood bicarbonate specific radioactivities when labelled propionate is infused intraruminally should be similar to the CO<sub>2</sub> ratio produced in the gluconeogenic cells of the liver. If propionate is infused intravenously into a peripheral site, there will be metabolism of propionate in peripheral tissues and the CO<sub>2</sub> ratio using blood bicarbonate specific radioactivities will not reflect the value of the CO<sub>2</sub> ratio of the tissues in the liver.

As glucose synthesis is restricted to gluconeogenic tissues, the glucose ratios for both acetate and propionate should reflect the metabolism of the gluconeogenic tissues. Therefore, using the glucose ratios and possibly the CO<sub>2</sub> ratio using propionate, it should be possible to obtain estimates of the percentage of the molecules in the oxaloacetate pool coming from cycling of the tricarboxylic acid cycle and thus to quantify the effects of metabolic crossover.

#### 4.5 METHOD USING BICARBONATE

##### 4.5.1 Introduction

The main sources of molecules in the dicarboxylic acid pools are

1. acids derived from cycling of the tricarboxylic acid cycle,

2. inputs from pathways that contain a carboxylation reaction,  
and
3. inputs from pathways that do not contain a carboxylation reaction.

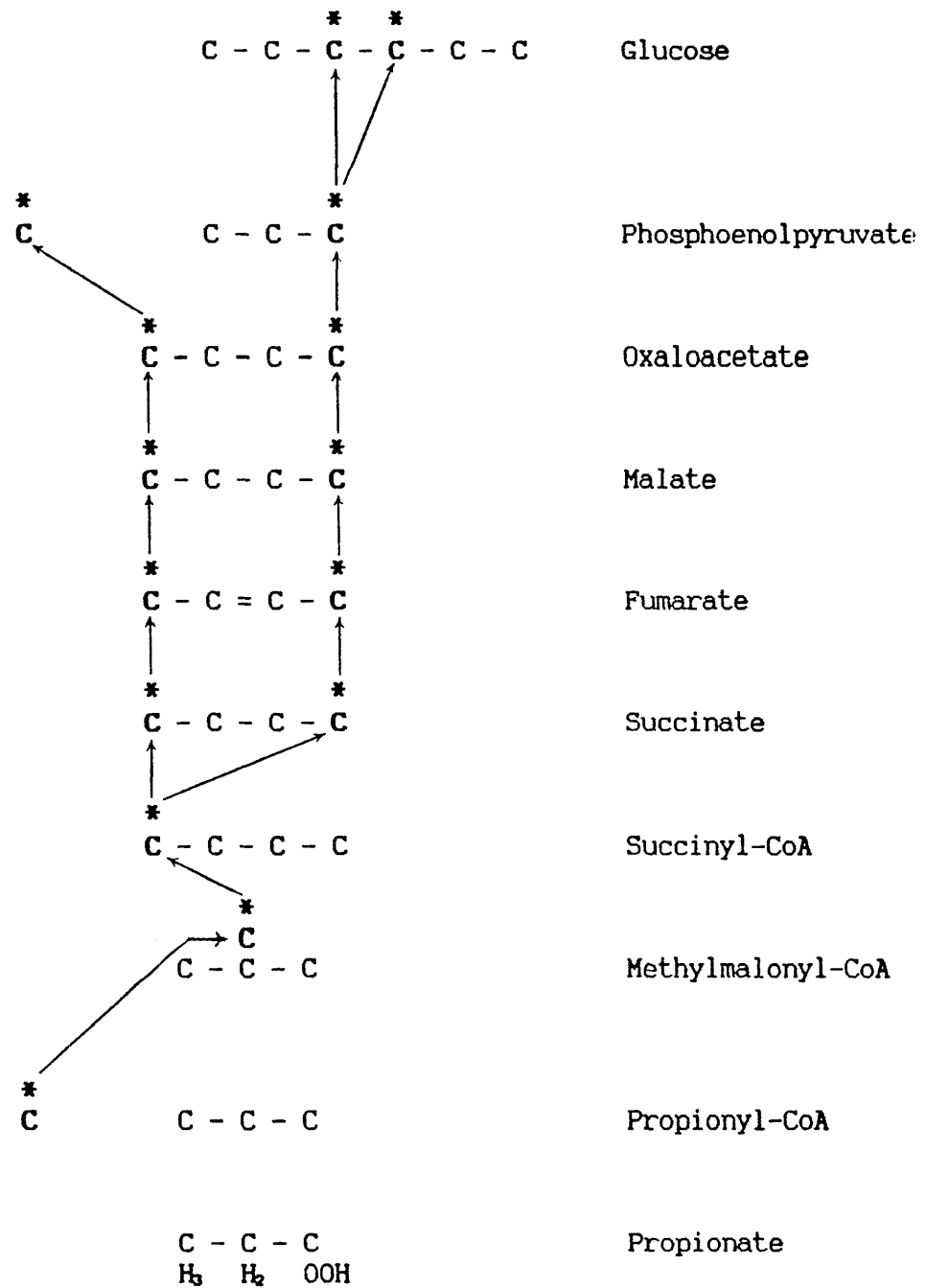
As most of the glucose precursors are 3 carbon units (e.g. propionate, lactate, alanine, pyruvate), the contribution of carbon from pathways that do not contain a carboxylation reaction is likely to be insignificant relative to the other sources of oxaloacetate. If this contribution is assumed to be zero, then by subtracting the percentage of the molecules in the oxaloacetate pool being provided by pathways containing a carboxylation reaction from 100%, an estimate of the percentage of the molecules in the oxaloacetate pool coming from cycling of the tricarboxylic acid cycle can be obtained. This method will overestimate the percentage of the molecules in the oxaloacetate pool coming from cycling of the tricarboxylic acid cycle by the percentage that comes from net input pathways that do not contain a carboxylation reaction.

#### 4.5.2 Incorporation Of $\text{HCO}_3^-$ Into Glucose

Although there is no net fixation of carbon from  $\text{HCO}_3^-$  into glucose, there is incorporation due to the symmetrical compounds in the pathway. When compounds that are first carboxylated pass through the symmetrical dicarboxylic acid pools, the carbon from bicarbonate becomes distributed about both carboxyl positions. Only one of these carboxyl carbons is removed between oxaloacetate and glucose. Figure 4-14 illustrates the pathway by which  $\text{H}^{14}\text{CO}_3^-$  is incorporated into glucose when propionate is the gluconeogenic precursor.

Figure 4-14

The positions of the carbon atoms in the intermediates which become labelled by  $H^{14}CO_2$  when propionate is converted directly to glucose.





Some metabolites , e.g. propionate, have to pass through the symmetrical dicarboxylic pools prior to being converted to glucose. Others, e.g. lactate, are carboxylated direct to oxaloacetate and, therefore, need not pass through a symmetrical compound on the way to glucose. However, there is evidence (eg. Hoberman and D'Adamo, 1960) that oxaloacetate is in complete isotopic equilibration with the symmetrical dicarboxylic acids. Therefore, most of the molecules that enter the dicarboxylic pools as oxaloacetate will equilibrate with the symmetrical compounds and thus cause the tracer to become distributed about both carboxyl carbons.

When glucose specific radioactivities are used to estimate the specific radioactivities of oxaloacetate, the extent of equilibration about the carboxyls is critical. This is because the carbon that is fixed in the carboxylation step is the carbon that is removed in the decarboxylation step if no equilibration occurs. The tracer from  $\text{CO}_2$  that is incorporated into glucose is the tracer that has equilibrated. Non-complete equilibration will result in the oxaloacetate specific radioactivity estimated from the glucose specific radioactivity being an underestimation of the average oxaloacetate carboxyl specific radioactivity. Thus, the percentage of the molecules in the oxaloacetate pool coming from sources that require carboxylation will be underestimated.

#### 4.5.3 Tracer From $\text{H}^{14}\text{CO}_3^-$ In The Tricarboxylic Acid Cycle

The carboxyl carbons of oxaloacetate are labelled by  $\text{H}^{14}\text{CO}_3^-$ . As discussed earlier, both carboxyls are removed in one turn of the tricarboxylic acid cycle, so no tracer in the carboxyl positions can return to the oxaloacetate pool via the tricarboxylic acid cycle.

#### 4.5.4 The Specific Radioactivity Of The Carboxyl Carbons Of Oxaloacetate Labelled By $H^{14}CO_3^-$

The reasoning used to develop equations for the specific radioactivity of the carboxyl carbon of oxaloacetate when  $[1-^{14}C]$ propionate or  $[1-^{14}C]$ acetate is infused can also be applied when  $H^{14}CO_3^-$  is infused. However, it is necessary to assume that there is complete equilibrium of tracer about the carboxyls of the dicarboxylic acids. Therefore,

$$OCSR = HCO_3SR \times \frac{1}{2} \times \frac{1}{(1+NHC03)}$$

where OCSR = specific radioactivity of the oxaloacetate carboxyl carbons.

$HCO_3SR$  = specific radioactivity of the carbon from  $H^{14}CO_3^-$  incorporated in the carboxylation reactions.

$NHC03$  = the proportion of the oxaloacetate pool formed from sources other than the carboxylation of three carbon compounds relative to the proportion formed from the carboxylation of three carbon compounds, the latter is defined as unity.

The factor  $\frac{1}{(1+NHC03)}$  is the proportion of the oxaloacetate pool provided by carboxylation of three carbon compounds. It accounts for the decrease in specific radioactivity caused by other sources of oxaloacetate.

The factor of  $\frac{1}{2}$  accounts for the randomization of the tracer about the carboxyl carbons of the symmetrical compounds.

The above equation can be rearranged to solve for NHC03:

$$\text{NHC03} = (\text{HCO3SR} / 2 \times \text{OCBR}) - 1$$

Thus the proportion of the oxaloacetate carboxyl carbons provided by pathways involving carboxylation reactions can be calculated. Under the assumptions discussed above (complete equilibration of the dicarboxylic acids and pathways that contain carboxylation reactions provide all net inputs to the tricarboxylic acid cycle), the oxaloacetate not provided by compounds that undergo carboxylation is provided by cycling of the tricarboxylic acid cycle. Non-complete adherence to the assumptions will result in this method overestimating the percentage of the molecules in the oxaloacetate pool provided by cycling of the tricarboxylic acid cycle.

#### 4.6 POSSIBLE TRACER FLOWS NOT SPECIFICALLY ACCOUNTED FOR IN THE THEORY USED TO DEVELOP THE EQUATIONS.

##### 4.6.1 Recycling Of Tracer Via Acetyl-CoA

It is possible for tracer on the middle carbons of oxaloacetate to return to the oxaloacetate pool via the following pathway: oxaloacetate, phosphoenolpyruvate, pyruvate, acetyl-CoA, citrate, then back to oxaloacetate via the tricarboxylic acid cycle. This pathway would occur if there were net oxidation of propionate or exchange of molecules between anabolic and catabolic pathways at the phosphoenolpyruvate pool in the appropriate compartment of the cells where gluconeogenesis is occurring.

This pathway of cycling would return all tracer from the middle carbons of oxaloacetate back to the oxaloacetate pool, though the tracer would be distributed equally on all four carbons. Tracer that was on the carboxyl carbons of oxaloacetate would not be returned; one carboxyl carbon would be removed in the oxaloacetate to phosphoenolpyruvate step and the other in the pyruvate to acetyl-CoA step.

Williamson, Scholz and Browning (1969) reported that acetyl-CoA inhibits pyruvate dehydrogenase and activates pyruvate carboxylase. The net effect of this is to increase the oxidation of two carbon units from fatty acids and to divert pyruvate from oxidation to glucose synthesis. Because ruminants absorb large amounts of acetate and butyrate, which can be metabolized through acetyl-CoA, it is expected that there would be little, if any, decarboxylation of pyruvate to acetyl-CoA in vivo. Freedman and Graff (1958) found that in fasted (i.e. needing to conserve glucose precursors) rats nearly all pyruvate entered the tricarboxylic cycle via carboxylation to oxaloacetate. As roughage fed ruminants need precursors for gluconeogenesis at all times, it was assumed in developing the equations presented earlier that cycling of tracer via the above pathway would have a negligible effect on the equations.

#### 4.6.2 Recycling Of Tracer Via Pyruvate

Another possible flow of tracer back to the oxaloacetate pool is via the following pathway; oxaloacetate, phosphoenolpyruvate, pyruvate, then directly back to oxaloacetate. Rognstad and Katz (1972) suggested that in rat kidney cortex the flux through pyruvate carboxylase and phosphoenolpyruvate carboxykinase may be twice the net

rate of glucose formation. Friedman, Goodman, Saunders, Kostos and Weinhouse (1971) using rat liver also suggested that there was a considerable amount of recycling through the above pathway.

Without futile cycling of carbon, the equivalent of six moles of ATP would be used per mole of glucose synthesised from lactate or pyruvate. Assuming a tightly coupled system, this corresponds to an oxygen consumption of 2g-atoms per mole of glucose formed (Soling and Kleineke 1976). Any futile cycling would result in an oxygen used/glucose synthesised ratio higher than two. Soling, Kleineke, Willms, Janson and Kuhn (1973) compared the oxygen used/glucose formed ratio in the isolated, perfused liver of rats, pigeons and guinea pigs and found very similar values in all three species. All were below 2.5. This suggests that the equivalent of 7 to 8 mole of ATP are required per mole of glucose formed. They concluded that futile cycling of carbon between phosphoenolpyruvate and pyruvate could not exceed 40% of the rate of pyruvate carboxylation. The combined effect of all the futile recycling only increases the energy requirements of gluconeogenesis by 15 to 30%.

Not all this is due to recycling of pyruvate by the above pathway. Some is due to futile cycling at the fructose-1,6-diphosphatase step and some due to the glucose-6-phosphate hexokinase/glucokinase step. It is therefore suggested that the amount of futile cycling at the pyruvate/oxaloacetate stage is not as large as the earlier work suggested. Mullhofer, Achwab, Muller, Von Stetten and Gruber (1977b) reported that under their experimental conditions there was no flow from phosphoenolpyruvate back to pyruvate. Part of the explanation of the earlier results probably lies in the reversibility of

phosphoenolpyruvate carboxykinase as discussed in the next section.

#### 4.6.3 Exchange Reactions Between Oxaloacetate And $\text{HCO}_3^-$

The work of Rognstad (1981) on the reversibility of phosphoenolpyruvate carboxykinase has considerable significance for the interpretation of isotope dilution data. He found that although  $\text{Mn}^{2+}$  had little effect on gluconeogenesis from lactate it caused the incorporation of  $^{14}\text{CO}_2$  into glucose to increase by 18%. He accounted for his results by suggesting that there was increased fixation of  $\text{CO}_2$  into the dicarboxylic acid pools due to isotope exchange in the reactions catalysed by pyruvate carboxylase and/or phosphoenolpyruvate carboxykinase. Since the malic enzyme can also fix  $\text{CO}_2$  into the dicarboxylic acids, the possibility that this enzyme is also stimulated by  $\text{Mn}^{2+}$  can not be completely ruled out.

In a following paper Rognstad (1982) found that there was considerable incorporation of  $\text{CO}_2$  into glucose, when glutamate was the substrate, even in the absence of added  $\text{Mn}^{2+}$ . This was unexpected because there is no  $\text{CO}_2$  fixation reaction in the direct pathway from glutamate to glucose. Adding  $\text{Mn}^{2+}$  increased the glucose specific radioactivity by about 50%. Adding an inhibitor of pyruvate carboxylase only slightly decreased the incorporation of  $\text{CO}_2$ . He suggested that  $\text{CO}_2$  was being fixed by exchange reactions in the phosphoenolpyruvate carboxykinase catalysed step and that this exchange was further stimulated by  $\text{Mn}^{2+}$ .

Because the experiments of Rognstad (1981,1982) were done on rats their applicability to the ruminant situation is unknown. However, considering the fundamental nature of the biochemistry involved, it is probable that the reactions do occur in ruminant tissues, at least to

some extent. Chang, Maruyana, Miller and Lane (1966) found using phosphoenolpyruvate carboxykinase purified from pig liver mitochondria that the oxaloacetate  $\text{HCO}_3^-$  exchange reaction was much more rapid than either the overall decarboxylation or carboxylation reactions. At pH 6.8, the relative carboxylation, decarboxylation and oxaloacetate  $\text{HCO}_3^-$  exchange rates were 1.0, 8.3 and 30 respectively. If this exchange reaction were to occur in ruminant tissues *in vivo* it would have a significant effect on the tracer flows and would have to be accounted for in the equations describing these tracer flows. If cycling of molecules in the tricarboxylic acid cycle cannot explain the results obtained in this thesis, this exchange reaction may have to be invoked to explain the data.

In the experiments of Rognstad (1982) the  $\text{CO}_2$  being incorporated into glucose in the absence of added  $\text{Mn}^{2+}$ , when glutamate is the substrate, is an overestimate of the exchange reaction between oxaloacetate and  $\text{HCO}_3^-$ . D'Adomo and Haft (1965), also using the isolated, perfused rat liver, estimated that between 40 and 60% of glutamate is metabolized to oxaloacetate by the alpha-ketoglutarate reductive pathway: glutamate, alpha-ketoglutarate, isocitrate, citrate, then to acetyl-CoA and oxaloacetate. If oxaloacetate formed in the cytosol does not equilibrate with the symmetrical dicarboxylic acids, the  $\text{CO}_2$  carbon incorporated into citrate when alpha-ketoglutarate is carboxylated is the carboxyl carbon of oxaloacetate incorporated into glucose. In the experiments of Rognstad (1982) this pathway would be contributing significantly to the flow of  $^{14}\text{CO}_2$  to glucose. Therefore, the extent of the exchange reaction remains unknown.

The alpha-ketoglutarate reductive pathway requires the enzyme citrate lyase to split the citrate to oxaloacetate and acetyl-CoA. This enzyme appears only to be active in the livers of mature ruminants when carbohydrate availability is high, eg. glucose infusions or concentrate feeding (Ballard, Filsell and Jarrett, 1972). In the livers of roughage fed animals the activity of citrate lyase appears to be virtually absent (Hanson and Ballard, 1967). Therefore, because only roughage fed animals were used in the experiments presented in this thesis the alpha ketoglutarate reductive pathway should be of negligible importance in gluconeogenic tissues.

#### 4.7 COMPARISON WITH THE WORK OF OTHER RESEARCHERS

In the past there have been several attempts (eg. Exton and Park, 1967; Heath, 1968) to derive the stoichiometry of carbon flows from tracer data. This involved the derivation of algebraic formulae that related the tracer data to carbon flows. More recent workers have had the advantage of the 'number crunching' ability of the digital computer and thus have been able to increase the complexity of the proposed schemes of metabolic interactions. For example, the scheme of metabolic interactions used by Crawford and Blum (1983) had 54 flux parameters (of which 34 were independent), 127 simultaneous linear equations and the specific radioactivity of each carbon atom in their scheme as the unknowns. However, no matter how complex the mathematical treatment of the data the validity of the solutions depends on the metabolic scheme actually representing the reactions and interactions that are actually occurring. Therefore, metabolic schemes developed for rats will not apply directly to ruminants because of known differences in metabolism (Ballard *et al.*, 1969). Unfortunately, the information available about the metabolism of



ruminants is considerably less than that for the metabolism of rats.

Thompson (1972) who worked with the lactating dairy cow, developed equations from which the percentage of the molecules in the oxaloacetate pool arising from cycling of the tricarboxylic acid cycle could be calculated. The reasoning used in this thesis (up to this stage) is very similar to that of Thompson (1972) (his stage two) because both are similar to that developed by Weinman et al. (1957). However, the present work does not contain the restrictive assumption that, one minus the proportion of the oxaloacetate pool arising from propionate represents the proportion of the oxaloacetate pool remaining in the cycle each turn to maintain the oxidation of acetyl-CoA. The present work also differs from that of Thompson (1972) in the adjustments to account for the effects of tracer recycling. In the work of Thompson (1972) the effects of recycling via the pathway; oxaloacetate, phosphoenolpyruvate, pyruvate, acetyl-CoA, citrate then back to oxaloacetate via the tricarboxylic acid cycle were considered, but the effects of recycling via oxaloacetate, phosphoenolpyruvate, pyruvate directly back to oxaloacetate and/or oxaloacetate/HCO<sub>3</sub><sup>-</sup> exchange reactions were not considered. In this work (Sections 6.5.4.4, 7.3.6 and 8.4.3), the latter forms of recycling are postulated to help explain the incorporation of CO<sub>2</sub> into glucose. As discussed in Section 6.5.4.4, these latter pathways decrease the incorporation of the carboxyl carbon of oxaloacetate into glucose and thus, affect the glucose ratio and the estimate of the proportion of the molecules in the oxaloacetate pool that arises from cycling of the tricarboxylic acid cycle.

The correction for the effects of metabolic crossover made by Wiltrout and Satter (1972) based on the incorporation of tracer into positions 3 or 4 of glucose during a [2-<sup>14</sup>C]propionate infusion is theoretically compatible with the interpretation used in this study. It is similar reasoning to that used by Weinman et al. (1957) in defining their glucose labelling ratio. However, Wiltrout and Satter (1972) made no attempt to correct for the effects of other forms of recycling.

The reasoning used by Hetenyi (eg. Hetenyi, 1982) is also theoretically compatible with the present work because it also is based on the work of Weinman et al. (1957). However, again no attempt has been made to account for other forms of recycling.

Goebel, Berman and Foster (1982) developed an elegant matrix that describes the steady state redistribution of carbon atoms by the tricarboxylic acid cycle. This model treats the individual carbon positions separately and defines pathways in terms of transition probabilities. However, the matrix is only valid for situations where the sequence of transition probabilities are the same as those given in their paper (Goebel et al., 1982). As the effects of some forms of recycling were not accounted for, the matrix cannot be used for situations where these forms of recycling are likely to occur (i.e. almost all situations).

There is a need to define and quantify the types and effects of recycling on the flow of tracer. When this is done the effects of the various forms of recycling can be incorporated into matrix models similar to that developed by Goebel et al. (1982). This would then allow more accurate and easier interpretation of the data obtained from isotope dilution experiments.

CHAPTER 5  
GENERAL MATERIALS AND METHODS

5.1 EXPERIMENTAL PROCEDURES

5.1.1 Experimental Animals

The sheep used were mature crossbreds or Merinoes weighing 30-35kg. They were housed indoors in metabolism cages under continuous lighting. All animals had had rumen fistulas established in them for at least 12 months.

5.1.2 Feeding Regime

The sheep were maintained on the experimental feeding regime for at least one month prior to the commencement of experiments. Their daily ration was given in equal portions at hourly intervals from an overhead, automatic moving belt feeder.

Only those animals that consumed their entire ration for two weeks preceding the sampling period were used in the experiments. In addition, only the results from animals that maintained their feed intake throughout the course of an entire infusion were used.

Water was supplied ad libitum.

### 5.1.3 Infusion Solutions

All isotopes were obtained from Amersham, International Ltd., England.

For intraruminal infusions, the isotope was diluted with water that had been boiled for at least 15 min, been made alkaline (10 drops/l of 10N NaOH) and had had the appropriate carrier added (approximately 0.002 mM/ml). All intravenous infusion solutions were made with sterile physiological saline (Travenol Laboratories Pty Ltd, Sydney, Australia). The isotope was added after the solutions had been made alkaline (except glucose solutions) and had had the appropriate carrier added.

During all infusions, subsamples of the infusion solutions were taken for analysis of radioactivity. The infusion solution subsamples were analysed by the same procedures as the biological samples.

### 5.1.4 Infusions

Tracer solutions were infused at a constant (accurately determined) rate, either intravenously at approximately 0.17ml/min or intraruminally at approximately 0.5ml/min using a peristaltic pump. The rate at which tracer was infused was measured during experiments by recording the weight loss from reservoirs over several intervals of about 2h. Silastic tubing was used to convey the tracer solution to the animal, where it was connected to either a jugular vein catheter or an infusion probe placed inside the rumen.

This infusion probe consisted of about 5cm of curved stainless steel tubing to which 5cm of polyethylene tubing (4mm I.D., 6mm O.D.) was attached. The curved metal tube was held rigidly in place by its tight fit through the rubber bung in the cannula. The infusion probe was directed cranially and thus away from the sampling probe.

#### 5.1.5 Jugular-vein Catheters

On the day preceding the administration of tracer, non-toxic polyethylene tubing (1.0mm I.D., Dural Plastics, Australia) was inserted into both jugular veins. The catheter for sampling was inserted about 25cm into a jugular vein and was in, or very close to, the heart. This allowed mixed venous blood to be collected. The catheter for administration of tracer was positioned about 10cm into the other jugular vein. Catheters were filled with 100 i.u./ml heparinized physiological saline overnight.

#### 5.1.6 Blood Sampling

Prior to taking each blood sample the heparin in the catheter was removed by withdrawing about 2ml of heparin and blood into a waste syringe. Blood was then drawn into a syringe with gentle even pressure. Excessive suction was avoided to prevent haemolysis of red blood cells. The catheters were then refilled with heparinized (25 i.u./ml) physiological saline.

#### 5.1.7 Rumen Fluid Sampling

The rumen fluid samples were obtained through a probe which consisted of a metal frame (5cm x 1cm x 1cm) covered with a double layer of fine nylon mesh. The frame was attached to a curved metal

tube (about 25cm long). The probe was positioned caudally in the rumen and held in place by its tight fit through the rubber bung in the cannula. The probe was flushed with about 10ml of rumen fluid 3 times before each sample was taken.

#### 5.1.8 Blood For Glucose Analysis

Blood for glucose analysis was immediately placed into heparinised (1 drop of 5000i.u./ml) centrifuge tubes, upturned gently to mix with the heparin, then chilled in ice. The red blood cells were separated from plasma by centrifuging at 3000g for 10min. The plasma was removed and stored at -17°C until analysed.

#### 5.1.9 Blood For $\text{HCO}_3^-$ Analysis

Five ml of blood was placed in a McCartney bottle. An inner tube containing 1ml of  $\text{CO}_2$  free 1N NaOH was inserted into the McCartney bottle and the lid replaced. One ml of 1N  $\text{H}_2\text{SO}_4$  was then injected through the lid into the blood to release the blood  $\text{CO}_2$ . The bottles were allowed to stand for at least 12h to trap the  $\text{CO}_2$  in the NaOH.

#### 5.1.10 Rumen Fluid For $\text{HCO}_3^-$ Analysis

Rumen fluid for  $\text{HCO}_3^-$  analysis was processed by the same procedures as were used for blood  $\text{HCO}_3^-$  analysis.

#### 5.1.11 Rumen Fluid For Volatile Fatty Acid Analysis

Fifteen ml of rumen fluid was placed in a McCartney bottle, 5 drops of conc  $\text{H}_2\text{SO}_4$  added and the bottle gently shaken. The sample was stored at -17° until analysed.

## 5.2 ANALYTICAL PROCEDURES

### 5.2.1 Dry, Ash And Organic Matter

Dry matter was analysed by drying the feed samples to a constant weight at 100°C (usually 24h was sufficient). The dried feed was milled through a 1mm screen and a subsample taken and ignited at 550-600°C for 3h to determine ash and organic matter.

### 5.2.2 Total Nitrogen

0.2g of the feed sample was oxidized by Kjeldahl oxidation using conc H<sub>2</sub>SO<sub>4</sub> and Se catalysts. The sample was made alkaline with sodium tetraborate (5% w/v), then steam distilled. The ammonia was collected into boric acid (2% w/v) and the ammonia-boric acid mixture titrated to pH5 (autoburette ABU12, Radiometer, Copenhagen) with 0.05N H<sub>2</sub>SO<sub>4</sub>. Recovery of ammonia nitrogen was checked using a standard (NH<sub>4</sub>)<sub>2</sub>SO<sub>4</sub> solution. All samples were adjusted to 100% recovery of nitrogen.

### 5.2.3 Volatile Fatty Acid Concentrations

Centrifuged rumen fluid (3000g for 10mins) was analysed for VFA concentrations and proportions by a gas-liquid chromatograph (Model 427, Packard Instrument Company, Illinois, USA) using isocaproic as an internal standard. The column used was a glass column, (1.83m long, I.D. 3.175mm) filled with acid washed Chromosorb W (60-80 mesh) beads (Johns-Manville, Celite Division, Denver, Colorado USA). The operating temperatures of the system were, injector 210°C, column 135°C and detector 180°C. The gas flows were, carrier nitrogen gas 60cc/min, hydrogen 40cc/min and air 400cc/min. The areas of the eluted peaks were integrated with a recording data processor (Model

604, Packard Instrument Company, Illinois, USA) attached to the chromatograph.

#### 5.2.4 Volatile Fatty Acid Specific Radioactivities

##### 5.2.4.1 Silicic Acid Column -

The method used was basically that of Leng and Leonard (1965). Two ml of centrifuged (3000g for 10min) rumen fluid was made alkaline with several drops of 10N NaOH and dried under reduced pressure over conc  $H_2SO_4$ . The dried residue was acidified, mixed with 1g silicic acid (Malinokrodt 100 mesh) and transferred to the top of a silicic acid column. The column had been prepared by mixing 5g of silicic acid with about 2.6ml of 0.25N  $H_2SO_4$ . The mixture was poured with n-hexane into a glass column (30cm x 1cm I.D.). The silicic acid settled on a plug of glass wool at the bottom of the column as the hexane eluted. The liquid flow rate and separation of the volatile fatty acids could be adjusted by altering the volume of 0.25N  $H_2SO_4$  mixed with the 5g of silicic acid.

The eluting solvent (hexane butanol) and mixing device were the same as used by Leng and Leonard (1965). The lower vessel contained 0.5% (v/v) butanol in hexane and the upper vessel 9% (v/v) butanol in hexane.

Five ml fractions of eluate were titrated under  $CO_2$  free conditions with approximately 0.02N NaOH in absolute ethanol, using 0.2% (w/v) bromothymol blue in absolute ethanol as an indicator. The normality of the NaOH was obtained by titrating against 2ml of standard HCl (0.020N). The three fractions containing the peak were collected without titration and bulked. One 5ml aliquot from the



bulked sample was titrated to determine the amount of acid present and a second 5ml aliquot was placed in a scintillation vial with 5ml scintillant (toluene containing 0.2% (w/v) PPO (2,5 diphenyloxazole) 0.02% (w/v) POPOP (1,4-bis-2 (5- phenyloxazolyl)-benzene) (Leng and Leonard, 1965) and counted for radioactivity.

One ml of infusion solution was diluted with approximately 50ml of alkaline water (the alkalinity was checked by adding 2 drops of bromothymol blue). To this a known amount of carrier acid was added. More 10N NaOH was added until the solution returned to alkalinity. This solution was made up to 100ml. Several 2ml aliquots were assayed for radioactivity by the same method as the samples. The carrier acid was calibrated by titrating several diluted samples against the NaOH used to titrate the samples.

Unless otherwise stated this method was used to determine the specific radioactivity of the volatile fatty acids.

#### 5.2.4.2 High Pressure Liquid Chromatography -

Volatile fatty acids were also isolated using a Waters (Waters Associates, Milford, Massachusetts USA) high pressure liquid chromatography system (U6K injector, M6000A and M45 pumps, M441 absorbance detector, 720 system controller). The column used was an Organic Acid Analysis Ion Exclusion column - Aminex HPX-87H (Biorad Laboratories, Richmond, California USA). The volatile fatty acids were eluted in the following manner: an initial isocratic period using 2.5% acetonitrile in 0.1% phosphoric acid was followed by a 5min period of increasing acetonitrile concentration (linear increase to 20% acetonitrile in 0.1% phosphoric acid). This concentration was maintained for 5min and then the column returned to the initial

concentration by a linear decrease in acetonitrile over the next 5min. The high concentration of acetonitrile caused the resin bed to swell and increase the pressure of the system, thus necessitating a further 30min interval to allow the pressure to return to the initial values. The temperature of the system was held at 30°C. At the operating flow rate (0.5ml/min) the pressure started at about 8000kPa and increased to about 10000kPa as the 20% acetonitrile was pumped through the column. Under the above procedure, propionate eluted at approximately 23min after injection. The areas of the eluted peaks were integrated using a recording data processor (Model 604, Packard Instrument Company, Illinois, USA). The eluted peaks were collected (approximately 1ml) in scintillation vials as they emerged from the detector. 10ml of scintillant (toluene:triton X 9:4 (v/v), 0.4% (w/v) PPO and 0.02% (w/v) POPOP) was then added to each vial.

Because an unknown substance in centrifuged rumen fluid eluted with propionate, a purification step was necessary. This was achieved by subliming the samples using thunberg tubes. Fifty ul of sublimed sample was injected onto the column.

The coefficient of variation of the specific radioactivity of propionate analysed by the high pressure liquid chromatography system method was 3%.

The results obtained from this method of determining the specific radioactivity of propionate were not significantly different from those obtained using the silicic acid column method.

### 5.2.5 HCO<sub>3</sub><sup>-</sup> Specific Radioactivity

The method is basically that of Leng and Leonard (1965). After at least 12h to allow the CO<sub>2</sub> to be absorbed, the inner tube was removed from the McCartney bottle, tipped into a bijou bottle and 1ml of 5% (w/v) NH<sub>4</sub>Cl added. The carbonate was precipitated as BaCO<sub>3</sub> by adding 0.4ml of 20% (w/v) BaCl<sub>2</sub>. The precipitate was plated, transferred to a weighed scintillation vial, dried at 100°C for 3h, cooled in a desiccator and reweighed. A glass bead was added and the samples ground to a fine powder by spinning on a vortex mixer. The powder was suspended in 10ml of scintillation fluid (3.4% (w/v) Cab-o-sil (Godfrey L. Cabot, INC., USA), 0.2% (w/v) POPOP and 0.4% PPO in xylene (Leng and Leonard, 1965)) using a rotary stirrer. Blanks were analysed with every run to check against CO<sub>2</sub> contamination of the 1N NaOH.

The NaH<sup>14</sup>C<sub>3</sub> infusion solution was assayed for radioactivity by adding 1ml to an alkaline, CO<sub>2</sub> free solution containing an accurately weighed quantity of dried Na<sub>2</sub>CO<sub>3</sub> (approx. 1g). The solution was made to volume (100ml) using CO<sub>2</sub> free water. Several 2ml aliquots of this diluted solution were taken through the same CO<sub>2</sub> transfer, BaCO<sub>3</sub> precipitation, and counting procedures as the samples. The activity in the infusion solution was obtained by multiplying the amount of carrier BaCO<sub>3</sub> by its measured specific radioactivity.

### 5.2.6 Glucose Specific Radioactivity

Plasma glucose concentration was determined using the auto analyser technique described by Frings, Ratliff and Dunn (1970). Later samples were analysed with a Glucose Rapid Test Kit on a Cobas Bio Centrifugal Analyser (both from F. Hoffmann - La Roche Co Ltd,

Diagnostica, Basle, Switzerland). The plasma was deproteinized by adding 5ml of  $\text{Ba}(\text{OH})_2$  (0.3N) and precipitating with approximately 4ml of  $\text{ZnSO}_4$  (0.3N). The glucose was extracted from the deproteinized plasma as the penta-acetate derivate (Jones 1965). This derivate was dissolved in 10ml of scintillation fluid (Toluene, 0.4% (w/v)PPO and 0.02% (w/v) POPOP) and counted. The infusion solution was diluted 1 in 100 and put through the same system as the samples.

#### 5.2.7 Scintillation Counting

All samples were counted in a Packard Tri-carb, Model 3255 (Packard Instrument Company, Illinois, USA). Blanks, prepared at the same time, with the same materials as the samples, were counted with the samples. All samples were counted for 10min or to at least 1000 counts above background.

Samples were corrected for quenching using the automatic external standard (AES) of the machine. The AES was calibrated to counting efficiency by regressing AES against the calculated counting efficiency of vials containing the appropriate scintillation cocktail and a known quantity of radiochemical disintegrations per minute. Except for the  $\text{BaCO}_3$  counting system, these vials were prepared from a diluted Standard  $^{14}\text{C}$  Toluene from Amersham International Limited. With the  $\text{BaCO}_3$  counting system, the vials were prepared with a known weight of standard  $\text{Ba}^{14}\text{CO}_3$  which had previously been calibrated against the standard  $^{14}\text{C}$  Toluene. The  $\text{BaCO}_3$  for this standardization was solubilized in 2ml of 0.2M tetra-sodium-EDTA and counted in 20ml of Miniria 20 (Koch-Light Laboratories Ltd).

### 5.3 MATHEMATICAL PROCEDURES

All mathematical calculations in this thesis were performed using at least four significant digits. This was because rounding of values used early in the complex, and often multi-stepped calculations may have resulted in an accumulation of errors owing solely to this rounding. Therefore, some of the values presented in the text may vary slightly from values calculated from the data (rounded to experimental accuracy) presented in the tables.

#### 5.3.1 Statistical Analysis

All statistical methods (i.e. means, standard deviations, standard errors, regression coefficients and test for homogeneity of straight lines) used were as described in Snedecor and Cochran (1967).

The coefficients of variation of both pump flow rates and radioactivity in the infusion solution were always less than 1.5%. Therefore, it was assumed that the coefficient of variation of the rate of tracer infusion was 2%.

It was assumed in the calculations that there was no covariance between parameters. Therefore, the variance (V) of X times Y was calculated by the approximation

$$(\text{mean}_x)^2 \times V_y + (\text{mean}_y)^2 \times V_x$$

The variance of X divided by Y was calculated by the approximation

$$\frac{(\text{mean}_x)^2}{(\text{mean}_y)^2} \times \left[ \frac{V_x}{(\text{mean}_x)^2} + \frac{V_y}{(\text{mean}_y)^2} \right]$$

### 5.3.2 Development Of The Models

A modelling approach is necessary to obtain accurate estimates of the rates of formation of metabolically related compounds when the rates of interconversion are high. The models constructed in this thesis use the general approach of Mann and Gurdipe (1966) with equations similar to those of Nolan et al. (1976). The Mann and Gurdipe (1966) approach formally recognizes the existence of an unlimited number of pools which may interchange material with the pools that are of interest, but still allows formulae to be derived from which rates of movement of tracee between specific pools of the system can be estimated. It is possible to solve any general, open compartment model with  $n$  pools using values obtainable in  $n$  different tracer experiments made, ideally, under identical conditions, provided each pool is the site of administration of tracer while it and all other pools are sampled (Nolan et al., 1976).

In the generalized open compartment model of  $n$  pools there are  $n^2 + n$  flows. Therefore,  $n^2 + n$  orthogonal equations have to be formulated so that values for the  $n^2 + n$  flows can be derived. The equations used to create the models were

1. Summation of flows of tracer from the system (for all infusions) = irreversible loss of tracer<sup>1</sup> ( $n$  equations)
2. Summation of flows of tracer around each of the non-infused pools (for all infusions) = 0 ( $n^2 - n$  equations)

---

<sup>1</sup> The infused pool specific radioactivity was expressed as 1.0 and the secondary pools as a proportion of this. Flows of material are obtained by multiplying the amount of material flowing along a pathway by the specific radioactivity of that material. When the specific radioactivity of the infused pool equals 1.0, the infusion rate of tracer equals the irreversible loss of tracee.

3. Summation of flows of tracee around each infused pool (for each infusion) = 0 (n equations)

Shown in Figure 5-1 is a set of equations for an infusion into a three pool model. Similar sets of equations were developed for all infusions in each model. Solutions to the sets of equations were obtained using a subroutine for solving simultaneous equations from the Numerical Algorithms Group (NAG) Fortran Library (F04ARF) on a DEC-system 2060 computer. In the models where flows were deleted, zeros for the deleted flows were substituted into all equations, thus, leaving more equations than unknowns. Solutions to the equations for these models could not be calculated via simultaneous equations and had to be calculated via a minimal least squares method (NAG Fortran Library FORJAF).

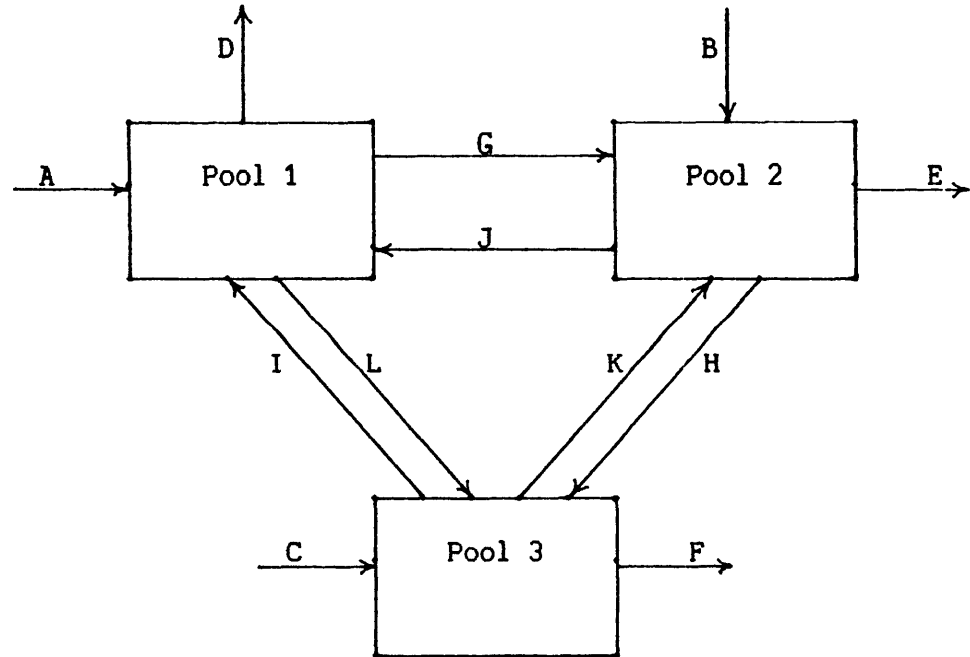
As all flows in a model have covariance with every other flow, an assessment of the experimental variation of each flow from the standard deviations of the inputs (irreversible losses and transfer quotients) would be virtually impossible (especially for the four and five pool models). Therefore, a 'monte carlo' (Sheppard, 1969) type technique was used. The standard deviation of every input was multiplied by a random normal deviate (0,1)<sup>1</sup> and added to the input values. A new set of solutions was then calculated. This procedure was repeated 100 times. An estimate of the variation of each flow was obtained by calculating the standard deviation of each flow generated by the 100 sets of solutions.

---

<sup>1</sup> A pseudo random real number from a normal distribution of mean zero and standard deviation of 1.0 was generated by NAG Fortran Library (G05DDF). The pseudo random number generator was set to a non-repeatable initial state by reference to a real time clock (NAG Fortran Library G05CCF). Thus, a different set of pseudo random real numbers were generated at each call to the generator.

**Figure 5-1**

An example of the equations used in developing the open system pool models. In the example, Pool 1 was the pool into which the tracer was infused.



Let,

1. The specific radioactivity of the pool into which tracer was infused (Pool 1) = 1.0.
2. The specific radioactivity of Pool 2 = 0.6. Therefore, the proportion of Pool 2 from Pool 1 = 0.6.
3. The specific radioactivity of Pool 3 = 0.3.

Therefore,

1. The loss of tracer from the system  

$$D + 0.6E + 0.3F = \text{the infusion rate of tracer}$$
2. The summation of tracer around the non-infused pools  

$$G + 0.3K - 0.6E - 0.6H - 0.6J = 0.0 \quad (\text{Pool 2})$$

$$L + 0.6H - 0.3F - 0.3I - 0.3K = 0.0 \quad (\text{Pool 3})$$
3. The summation of tracee around the infused pool  

$$A + I + J - D - G - L = 0.0$$

Similar equations were developed when tracer was infused into Pools 2 and 3. The same procedure was also used in developing equations for the 2, 4 and 5 pool models.